Integrative analysis of C. elegans modENCODE ChIP-seq datasets to infer transcription factor-responsive targets and upstream regulators of differentially-expressed genes from expression profiling experiments

Eric L Van Nostrand and Stuart K Kim

Genome Res. published online March 26, 2013
Access the most recent version at doi:10.1101/gr.152876.112

Integrative analysis of *C. elegans* modENCODE ChIP-seq datasets to infer transcription factor-responsive targets and upstream regulators of differentially-expressed genes from expression profiling experiments

Running title: Integrative ChIP-seq analysis in *C. elegans*

Eric L. Van Nostrand [1,2] and Stuart K. Kim [1]*

1. Department of Genetics and Department of Developmental Biology, Stanford University Medical Center, Stanford, CA 94305, United States
2. Current address: Department of Cellular & Molecular Medicine, University of California at San Diego, La Jolla, CA, 92037

***** Corresponding author: Stuart K. Kim, stuartkm@stanford.edu, (650-725-7671)

Abstract

The C. elegans modENCODE consortium has defined *in vivo* binding sites for a large array of transcription factors by ChIP-seq. In this paper, we present examples that illustrate how this compendium of ChIP-seq data can drive biological insights not possible with analysis of individual factors. First, we analyze the number of independent factors bound to the same locus, termed transcription factor complexity, and find that low-complexity sites are more likely to respond to altered expression of a single bound transcription factor. Next, we show that comparison of binding sites for the same factor across developmental stages can reveal insight into the regulatory network of that factor, as we find that the transcription factor UNC-62 has distinct binding profiles at different stages due to distinct cofactor co-association as well as tissue-specific alternative splicing. Finally, we describe an approach to infer potential regulators of gene expression changes found in profiling experiments (such as DNA microarrays) by screening these altered genes to identify significant enrichment for targets of a transcription factor identified in ChIP-seq datasets. After confirming that this approach can correctly identify the upstream regulator on expression datasets for which the regulator was previously known, we applied this approach to identify novel candidate regulators of transcriptional changes with age. The analysis revealed nine candidate aging regulators, of which three were previously known to have a role in longevity. We experimentally showed that two of the new candidate aging regulators can extend lifespan when over-expressed, indicating that this approach can identify novel functional regulators of complex processes.

Introduction

The development of chromatin immunoprecipitation followed by quantification by microarray (ChIP-chip) or high-throughput sequencing (ChIP-seq) has enabled the identification of transcription factor binding sites *in vivo* (Ren et al. 2000; Johnson et al. 2007). These DNA sites bound by transcription factors can be used to characterize DNA binding motifs, identify novel regulated targets, and understand its biological function through analysis of its targets (Spitz and Furlong 2012; Wang et al. 2012). Identification of targets for factors that play cooperative roles during development can provide insight into the redundant and specific functions of the individual factors, as well as the molecular mechanisms through which multiple factors interact to regulate gene expression (reviewed in (Spitz and Furlong 2012)).

The *C. elegans* modENCODE consortium has generated 98 ChIP-seq datasets identifying directly-bound targets for 57 transcription factors in one or more developmental stages (Zhong et al. 2010; Niu et al. 2011) (Supplemental Table 1). Similar efforts by the ENCODE and modENCODE consortia as well as efforts from individual laboratories have identified targets bound by hundreds of transcription factors in human, mouse, and fly (MacArthur et al. 2009; Negre et al. 2011; Garber et al. 2012; Gerstein et al. 2012). Compendia of ChIP-seq datasets can be used to construct regulatory networks, and to find novel pairs of transcription factors with similar sets of bound targets that suggest new cases of transcription factor co-association (Niu et al. 2011; Gerstein et al. 2012). Additionally, in combination with datasets describing histone modifications and other measures of chromatin state, such compendia can be used to predict gene expression (Cheng et al. 2011; Cheng et al. 2012; Marbach et al. 2012). These examples illustrate how combining data for many transcription factors can provide emergent insights about gene regulation that cannot be found by studying one factor by itself.

Efforts to profile transcription factor binding by the ENCODE and modENCODE consortia, as well as by many groups, have revealed a high degree of overlap between the binding sites of different transcription factors ((Gerstein et al. 2010; Roy et al. 2010; Garber et al. 2012), reviewed in (Biggin 2011)). Studies of transcription factor complexity, defined as the total number of transcription factors bound to each genomic region, have revealed that Highly Occupied Target (HOT) regions (bound by many transcription factors) and low-complexity regions (bound by one or only a few factors) are functionally different in many ways (Gerstein et al. 2010; Roy et al. 2010; Garber et al. 2012). Low-complexity binding sites are often enriched

for DNA binding motifs of the bound transcription factor, suggesting that the transcription factor directly binds to DNA. In contrast, high-complexity sites often show weaker or no enrichment for the DNA binding motifs of bound transcription factors, suggesting that the transcription factors may instead associate with the region through protein-protein interactions (Moorman et al. 2006; Gerstein et al. 2010; Roy et al. 2010; Yip et al. 2012). HOT regions are also associated with histone modification profiles and chromatin signatures characteristic of open chromatin in human and *D. melanogaster*, with strong enhancer activity in *D. melanogaster*, and with essential genes with high levels of expression and ubiquitous expression across tissues in *C. elegans* (Gerstein et al. 2010; Negre et al. 2011; Kvon et al. 2012; Yip et al. 2012).

In this work, we further explore how integration of multiple ChIP-seq datasets can enable insights not possible from a single ChIP experiment. First, we address the question of how to identify the subset of ChIP-seq targets that are likely to be factor-responsive. Often, only a subset of targets that are directly bound by a transcription factor are observed to change expression upon either an increase or decrease in the activity of that transcription factor (e.g., an average of 58% of ChIP-seq targets for 37 transcription factors in yeast (Gao et al. 2004), 26% of NANOG targets and 50% of POU5F1 targets in mice (Loh et al. 2006), and ~10% of *hlh-1* targets in *C. elegans* (Kuntz et al. 2012); reviewed in (Spitz and Furlong 2012)). By analyzing ChIP-seq data in combination with datasets describing genes altered upon single transcription factor perturbation, we find that low-complexity ChIP-seq targets are more likely to be factor-responsive than high-complexity targets.

Second, we use the large number of datasets to identify transcription factors that have different sets of targets identified in multiple developmental stages. Analysis of the low-complexity targets for one such transcription factor, UNC-62/Homothorax, enabled us to characterize two mechanisms by which it may associate with distinct targets in different tissues: tissue-specific alternative isoforms, and differential co-association with LIN-39/HOX.

Third, we show that a compendium of ChIP-seq datasets can be used to screen for candidate regulators that bind to the upstream regions of genes that change expression in an expression profiling experiment. We validated this approach by using previously published gene expression profiling data to show that HLH-1 and SKN-1 can be correctly identified as transcription factors that bind to the upstream regions of genes responsive to *hlh-1* and *skn-1*, respectively. We then applied this approach to find candidate upstream regulators of age-

regulated genes and identified nine transcription factors, five of which extend lifespan in either over-expression or knockdown experiments.

Results

Efforts to experimentally identify direct targets of transcription factors have revealed an unexpected degree of complexity among transcription factor binding sites (Gerstein et al. 2010; Roy et al. 2010; Garber et al. 2012). To explore the distinct functions of low- and high-complexity binding sites, we performed analysis on 98 ChIP-seq datasets generated by the *C. elegans* modENCODE consortium that identify direct binding sites for 57 transcription factors (Supplemental Table 1). For each ChIP-seq binding site, we defined complexity as the maximum number of transcription factors that are bound within that genomic region (Roy et al. 2010; Garber et al. 2012). We observed a wide range of binding events; for example, a DNA site in the *pat-3* promoter (a previously characterized target of HLH-1 (Fukushige et al. 2006)) has HLH-1 binding sites that are bound by three, eight, and sixteen other transcription factors (~5%, 14%, and 28% of the 57 factors considered). In contrast, the promoter region of translation elongation factor 1-alpha homolog *eef-1A.1* and RFC (DNA replication factor) family gene *rfc-4* contains a region bound by 44 different transcription factors (77%) (Fig. 1A,B). The 98 ChIP-seq datasets showed a wide range of complexity profiles, ranging from experiments in which more than half of binding sites are bound by eight or less total transcription factors to those with more than half bound by 38 or more transcription factors (Supplemental Table 1).

HOT regions

Previously, 304 Highly Occupied Target (HOT) regions were defined as those bound by 15 or more out of 23 transcription factors (Gerstein et al. 2010). We re-annotated HOT regions as 296 regions bound by 38 or more of the 57 assayed transcription factors (>65%, equivalent to the previous definition) (Fig. 2A, Supplemental Datafile 2). We observed that HOT regions tended to be positioned close to the transcriptional start site of genes, unlike regulatory enhancers that can act at a long distance (Krivega and Dean 2012); specifically, 83% of HOT regions were within 1000 bp of the transcriptional start site, whereas only 59% of low-complexity binding sites (with 8 or less factors bound) were located within 1000 bp of the transcriptional start site ($p < 10^{-10}$ by Fisher's Exact test)(Fig. 2B).

We found that many specific gene classes were over-represented among HOT-associated genes, including SL2 transcripts, snoRNA transcripts, and genes encoding ribosomal subunit proteins (each $p < 10^{-5}$ by Fisher's Exact test). Gene Ontology analysis indicated enrichment for genes involved in multiple aspects of embryonic and larval development as well as reproduction (Supplemental Table 2), consistent with the previous finding that HOT-associated genes are expressed at a high level, expressed ubiquitously in all tissues, and have essential functions (Gerstein et al. 2010). In contrast, genes that are highly expressed at only specific points in the worm life-cycle, such as vitellogenin and collagen genes, were not associated with HOT regions (0 out of 6 and 0 out of 159 respectively).

Low-complexity targets tend to respond to altered transcription factor expression

Next, we asked whether binding site complexity was predictive as to whether the expression of a target gene was altered in response to changes in a bound factor. For this analysis, we selected two transcription factors (HLH-1 and SKN-1) with binding targets characterized from ChIP-seq experiments and responsive genes identified from over-expression or knockdown expression experiments. The first, HLH-1, is a helix-turn-helix transcription factor that is the *C. elegans* ortholog of MYOD1 and is a key regulator of muscle differentiation and development, (Fukushige and Krause 2005; Lei et al. 2009). Previous experiments identified 2128 genes that were significantly induced upon over-expression of HLH-1 in early embryos (Fukushige et al. 2006; Fox et al. 2007), and ChIP-seq experiments from modENCODE indicate that HLH-1 binds to 4191 genes in mixed embryos (Niu et al. 2011). The second, SKN-1, is a bZIP-domain containing transcription factor that is orthologous to NRF1/2/3. SKN-1 plays roles in specification of intestinal, muscular, and pharyngeal cell fates of the EMS blastomere and in the response to oxidative stress (Bowerman et al. 1992; Maduro et al. 2001; An and Blackwell 2003; Tullet et al. 2008). DNA microarray experiments profiling *skn-1* knockdown in worms exposed to oxidative stress identified 91 SKN-1-responsive genes (Park et al. 2009), and modENCODE ChIP-seq datasets identified sites bound by SKN-1 associated with 3572 genes in L1 stage larvae and 3131 genes in L2 stage larvae (with q-value $\leq 10^{-5}$)(Niu et al. 2011). For each, binding sites were associated with genes if they were located within the gene body, or within 5kb upstream of the annotated transcription start site (see Methods).

Using these datasets, we asked whether the complexity score for an HLH-1 or SKN-1 binding site correlated with factor-responsive targets. First, we determined the overlap between the list of HLH-1-activated genes and the set of genes with HLH-1 binding sites with complexity of at most *n*, with *n* ranging from 1 to 57 factors associating to the same genomic locus. We observed that low-complexity sites tended to be associated with genes that were HLH-1-responsive, whereas inclusion of intermediate- and high-complexity sites yielded fewer HLH-1-responsive targets (Fig. 3A, Supplemental Fig. 1A). Using the Matthews correlation coefficient to optimize the trade-off between the increased percent of HLH-1-responsive genes at low complexity thresholds and the increased number of targets when intermediate- and high-complexity sites are included, we found that a complexity score of 8 provided the optimal threshold for HLH-1 (Fig. 3A). Using this cutoff, 39.5% (591) of the 1496 genes associated with HLH-1 binding regions with a complexity score of 8 or less were activated by HLH-1 (3.1-fold enriched, $\chi^2 = 1047$). This was a 99% improvement over regions with a complexity score of 9 or more, and a 49% improvement over using all HLH-1 binding sites, which were only 1.6-fold and 2.1-fold enriched ($\chi^2 = 132$ and 789), respectively (Fig. 3B).

Next, we applied the same complexity criteria to determine whether the complexity of SKN-1 binding sites was also correlated with responsiveness to decreased activity of *skn-1*. The first SKN-1 ChIP-seq dataset (from L2 larvae) identified 579 low-complexity targets and 1668 intermediate- and high-complexity targets bound by SKN-1. We found that genes associated with the low-complexity sites showed a 4.8-fold enrichment for activation by SKN-1 ($p = 6.3\text{x}10^{-22}$ by Chi-square test). In contrast, the intermediate- and high-complexity targets were not significantly enriched for *skn-1* responsive genes (Fig. 3C).

We obtained a similar result for the second SKN-1 ChIP-seq dataset (from L1 larvae), which has 344 low-complexity and 2301 intermediate- and high-complexity targets. Although this set showed surprisingly low overlap with the ChIP-seq performed in L2 larvae (only 16% of L1 low-complexity binding sites also bound in L2 larvae), SKN-1 (L1) low-complexity targets still showed a 4.3-fold enrichment for activation by SKN-1 ($p = 7.5\text{x}10^{-7}$)(Fig. 3D). In contrast, neither intermediate- and high-complexity targets nor all SKN-1 (L1) targets were significantly enriched for *skn-1*-activated genes. Thus, without incorporating information from the 97 other ChIP-seq datasets, analysis of the SKN-1 (L1) ChIP-seq dataset on its own would not show any enrichment for *skn-1*-responsive genes. Additionally, these results indicate that the complexity

criteria trained using the HLH-1 datasets can be applied to analysis of other transcription factors. Training using the SKN-1 datasets themselves gave a different cutoff for maximal correlation, but showed the same anti-correlation between binding site complexity and factor-responsive expression (Supplemental Fig. 1B). The number of transcription factors bound to each base in the *C. elegans* genome is listed in Supplemental Datafile 1 to enable incorporation of binding site complexity in future analyses.

In addition to binding site complexity, a gene can be regulated by many transcription factors binding to multiple distinct sites. However, we found that incorporation of gene-level complexity did not improve the ability to distinguish factor-responsive from non-responsive targets compared to incorporation of binding site-level complexity (Supplemental Fig. 1C). This result suggests that the correlation of binding site complexity with factor-responsive targets is not simply due to the number of transcription factors associated with the entire gene promoter.

Tissue-specificity of transcription factor targets

Next, we explored whether the target genes bound by a transcription factor were enriched for expression in the tissue where the factor is known to be expressed. We obtained lists of genes with expression significantly enriched in a variety of tissues (e.g. intestine or neurons) and tissue sub-types (e.g. A-class neurons)((Roy et al. 2002; Zhang et al. 2002; Colosimo et al. 2004; Fox et al. 2005; Pauli et al. 2006; Von Stetina et al. 2007; Spencer et al. 2011), listed in Supplemental Table 3). For each list of tissue-enriched genes, we performed pair-wise comparisons with low-complexity targets from every ChIP-seq dataset, identifying many significant transcription factor target – tissue pairings (Supplemental Fig. 2). To test this approach, we identified thirteen factors that had a high correlation with at least one tissue-enriched gene list and had expression patterns described in WormBase (Harris et al. 2010). In twelve of the thirteen cases, the targets were enriched for expression in a tissue in which the transcription factor was expressed (Supplemental Fig. 3).

Tissue-specific gene regulatory networks controlled by UNC-62 Homothorax

Although modENCODE ChIP-seq experiments were performed using whole worms, binding of a transcription factor to distinct target genes in different developmental stages could occur if the factor was expressed in one tissue at one stage but another tissue at a later stage, or

acted with different co-factors in the different stages. We identified four transcription factors (PHA-4, FOS-1, SKN-1, and UNC-62) for which targets identified in different developmental stages were enriched for expression in different tissues. We analyzed one of these transcription factors (UNC-62) as a proof-of-principle that one can use genomic analyses to uncover potential underlying molecular mechanisms responsible for binding site specificity.

UNC-62 is the ortholog of Homothorax/Meis, and is a co-factor of the HOX transcription factor LIN-39. *unc-62* is involved in the development of the nervous system, hypodermis, and vulva as well as in aging, and acts through both HOX-dependent and HOX-independent functions ((Van Auken et al. 2002; Yang et al. 2005; Curran and Ruvkun 2007; Jiang et al. 2009; Potts et al. 2009; Van Nostrand et al. 2013)). An alternative splicing event in *unc-62* produces two transcripts that include either exon 7a or 7b, encoding alternative amino termini of the DNA-binding TALE homeodomain (Van Auken et al. 2002). Using isoform-specific fluorescent reporters UNC-62(7a) was observed to be predominantly expressed in the intestine starting at the L3 larval stage and continuing through adulthood, whereas UNC-62(7b) was expressed in neurons, the ventral nerve cord, vulval precursor cells, and hypodermis beginning in embryos and continuing through adulthood (; Fig. 4A) (Van Nostrand et al. 2013).

The modENCODE consortium performed UNC-62 ChIP-seq experiments in L1, L2, and L3 larvae (which express only *unc-62(7b)*; see Supplemental Fig. 4) as well as young adults (which express both *unc-62(7a)* and *unc-62(7b)*). We identified 7 low-complexity UNC-62 binding sites in L1 larvae, 47 in L2 larvae, 231 in L3 larvae, and 339 in young adults; due to the low number of targets, we removed the L1 dataset from additional analyses. We observed that UNC-62 showed a dramatic shift in binding between L2/L3 larvae and adults; 62% of UNC-62 L2 peaks overlapped regions enriched in L3, but only 13% of L2 peaks and 5% of L3 peaks were enriched in young adults (Fig. 4B).

We performed three comparisons of the binding targets of UNC-62 in the L2/L3 stages to the young adult stage: overlap with binding sites of co-factor LIN-39, tissue-specific expression of target genes, and differential motif enrichment. First, we found that 45% of low-complexity UNC-62 binding sites in L2 larvae and 42% of low-complexity L3 binding sites overlapped low-complexity LIN-39 binding sites, reflecting the known shared functions of UNC-62 and LIN-39 during these larval stages. By contrast, only 2% of low-complexity UNC-62 young adult binding sites were also bound by LIN-39, indicating that these transcription factors likely have divergent

roles at this stage (Fig. 4B). Second, we found that UNC-62 low-complexity targets in the L2 and L3 larval stages were enriched for genes with neuronal expression, similar to HOX LIN-39 targets in the L3 larval stages (Fig. 4C). In contrast, the UNC-62 young adult targets were enriched for genes expressed predominantly in the intestine. These profiles match the expression of the isoforms of *unc-62*, as *unc-62(7a)* is expressed in the intestine in young adults, and both *unc-62(7b)* and *lin-39* are expressed in neuronal tissues (as well as other tissues) in larvae (Fig. 4A; (Wagmaister et al. 2006)).

Third, we performed a *de novo* search to identify DNA motifs contained within the UNC-62 peaks using the central 100 nt region of low-complexity UNC-62 binding sites in L3 and young adults. We identified two similar motifs: 1) a motif with consensus sequence GTGACA that is enriched in both the L3 and the young adult stages (2.8-fold, p = 0.0007 for the L3 stage and 3.4-fold, p = 1.3×10^{-7} for the young adult stage), and 2) a motif with consensus sequence TTGACA motif that was significantly enriched in young adult (3.3-fold, p = 1.5×10^{-22}) but not in the L3 larval stage (1.7-fold enriched relative to flanking regions, p > 1 after Bonferroni correction; 2.0-fold enriched, $p = 5.6 \times 10^{-5}$ in young adult binding sites relative to L3 binding sites) (Fig. 4D). Both motifs contain the core TGACA sequence previously described as the binding site for *Drosophila* Homothorax (Noyes et al. 2008).

In summary, these results suggest that multiple mechanisms may direct stage-specific binding of UNC-62 to its targets: 1) differential use of the LIN-39 co-factor in specifying binding targets in neurons compared to the intestine, and 2) binding to distinct DNA motifs by the UNC-62(7a) versus the UNC-62(7b) isoform. Similar analysis could suggest mechanisms for tissue specificity for additional factors that could be dissected with further experimental exploration.

Identifying upstream transcription factors involved in regulating gene expression changes from genome-wide profiling experiments

A commonly-arising question in high-throughput gene expression profiling experiments is to identify upstream transcriptional regulators that may be responsible for causing the observed transcriptional differences. Given the increasing availability of ChIP-seq datasets describing transcription factor targets, one approach to find such candidate regulators is to search for transcription factors that bind to the upstream regions of differentially-expressed genes

(Lachmann et al. 2010; Zambelli et al. 2012). Rather than test all of the targets from the ChIP-seq experiments, we use only the low-complexity targets as this subset is enriched for factor-responsive targets.

To test the validity of this approach, we analyzed four expression profiling experiments: 1) genes induced following over-expression of HLH-1, 2) genes decreased upon knockdown of SKN-1, 3) genes decreased upon knockdown of UNC-62, or 4) genes that have altered expression during aging. We chose the first three datasets as positive controls, as the upstream regulator was present in the modENCODE database. For the fourth dataset, we chose aging as a complex process for which transcriptional changes are likely the effect of altered activity of multiple regulators.

For HLH-1, we compared the set of 2128 HLH-1-activated genes to low complexity target genes from each of the 98 ChIP-seq datasets, and found that HLH-1 ChIP-seq dataset was the most significantly enriched for genes that change expression upon HLH-1 over-expression (3.1-fold enriched, p-value < 10^{-100}, χ^2 = 1047)(Fig. 5A). For SKN-1, we performed a similar analysis on the 91 genes that decrease expression following *skn-1* knockdown (Park et al. 2009). Out of 98 ChIP-seq datasets, the top two were SKN-1 ChIP-seq datasets (4.8-fold enriched, p = $6.3\text{x}10^{-22}$ in the L2 larval stage and 4.3-fold enriched, p = $7.5\text{x}10^{-7}$ in the L1 stage respectively)(Fig. 5B). For the SKN-1 ChIP-seq experiment using L1 worms, analysis using all binding sites does not show enrichment for genes responsive to *skn-1* knockdown, indicating that SKN-1 is only identified as an upstream regulator of genes responsive to SKN-1 when low binding site complexity is incorporated (Supplemental Fig. 5C; as discussed in Fig. 3D).

However, when we compared the ChIP-seq datasets against 115 genes that are activated by and 67 genes repressed by UNC-62 in young adults (Van Nostrand et al. 2013), neither stage-matched UNC-62 ChIP-seq targets from young adult worms nor UNC-62 targets in the L2 or L3 stage showed significant overlap (Fig. 5C, Supplemental Fig. 5D). This false negative result may reflect that knock-down of *unc-62* activity results in expression changes of a small number of direct targets, which subsequently leads to a cascade of gene expression changes of secondary indirect targets. Thus, the degree to which transcriptional changes are comprised of primary, direct targets instead of secondary, indirect ones represents a limitation for this approach.

A potential confounding factor is that the significance level depends on the number of genes identified in the ChIP-seq experiments, which would undesirably favor ChIP-seq

experiments with a large number of targets. To address this concern, we developed a method using a Naïve Bayes classifier, in which each binding site is given a RP (Responsiveness-Predictor) score as a function of both its complexity as well as its significance *q*-value (see Methods). We then selected the top scoring 500 sites in order to compare an equal number of binding sites from each ChIP-seq dataset against each other as described above.

First, we independently trained a model to predict targets that are induced by HLH-1 over-expression for each ChIP-seq dataset. Similar to before, we observed that the HLH-1 ChIP-seq dataset was the best of all of the modENCODE ChIP-seq datasets at predicting *hlh-1*-induced genes; specifically, the top 500 HLH-1 binding sites were 4.5-fold enriched for induction by *hlh-1* (p-value < 10^{-100}, $\chi^2 = 761$)(Supplemental Fig. 5A-B). Next, we asked whether RP scores (trained to weight ChIP-seq parameters using HLH-1 data) could be used to infer regulators for the SKN-1 dataset. Consistent with the earlier results, we observed that the only datasets showing significant enrichment were the two SKN-1 ChIP-seq datasets; specifically, SKN-1 targets in L1 larvae were 3.6-fold enriched ($p = 7.9\text{x}10^{-9}$) and those in L2 larvae were 5.1-fold enriched ($p = 9.8\text{x}10^{-9}$) for *skn-1*-activated genes (Fig. 5D). This method did not, however, improve the correlation between UNC-62 binding and *unc-62*-responsive expression (Supplemental Fig. 5E).

In summary, our analysis correctly identified the *hlh-1* and *skn-1* transcription factors as upstream regulators of genes that change expression following *hlh-1* over-expression or *skn-1* knock-down, respectively. These results indicate that it is possible to identify upstream regulators *in silico* from a gene expression profiling experiment by screening ChIP-seq datasets. In one case (SKN-1 in L1 larvae), the upstream regulator is only identified once binding site complexity is incorporated.

Identification of novel aging regulators

Encouraged by the success of using ChIP-seq data to infer upstream transcriptional regulators for gene signatures in two out of three cases, we turned to analysis of genes that change expression during aging. To screen for putative aging regulators, we compared each set of transcription factor targets against 1106 genes with altered expression during aging (Budovskaya et al. 2008). We performed this screen using both scoring methods: 1) only those binding sites with low-complexity (Fig. 6A), and 2) using the 500 binding sites with the highest

RP scores for each ChIP-seq dataset (Fig. 6B). The two approaches are complementary, as the first uses only significant binding peaks (even if they are few in number) whereas the second uses an equal number of binding sites across datasets in order to improve sensitivity for datasets with fewer binding sites (but may include sites bound weakly by the transcription factor). We identified nine transcription factors that are significantly enriched for binding to age-regulated genes with at least one of the two methods; six of the nine were significantly enriched using both methods.

Modulation of the activity of three of the nine (ELT-3, UNC-62 and SKN-1) has previously been shown to increase lifespan. ELT-3 is involved in age-regulated changes in the hypodermis, and increased expression of ELT-3 (via knockdown of repressors ELT-5 or ELT-6) extends lifespan (Budovskaya et al. 2008). HOX co-factor UNC-62 is involved in age-regulated changes in the intestine, and *unc-62* knockdown in adults increases lifespan (Curran and Ruvkun 2007). SKN-1 is involved in mediating the oxidative stress response, and over-expression of an activated form of SKN-1 increases lifespan (Tullet et al. 2008; Przybysz et al. 2009).

To validate the role of the remaining six candidate aging regulators (*nhr-28*, *pqm-1*, *fos-1*, *C01B12.2*, *nhr-77*, and *nhr-76*), we asked whether increasing or decreasing their activity can increase lifespan. We first performed RNAi to determine if reduction in activity increased lifespan. We confirmed that knockdown of *unc-62* in adults can significantly extend lifespan as reported previously (Curran and Ruvkun 2007), but did not observe reproducible extension of lifespan for any of the novel candidates (Supplemental Table 4).

To assay the lifespan phenotype of over-expression, we obtained a transgenic strain from the modENCODE consortium that carries a low-copy randomly integrated fosmid that contains the desired transcription factor (with a C-terminal GFP tag), additional flanking genes as described below, and rescue marker *unc-119*. Strains containing fosmids including *pqm-1*, *fos-1*, *C01B12.2*, or *nhr-77* had wild-type lifespan (Supplemental Table 5), whereas strains containing either the *nhr-28* or the *nhr-76* fosmid showed significant extension of lifespan (15-30% and 6-15%, respectively; each $p < 0.01$ by log-rank test in three independent experiments)(Fig 6C-D).

The first new candidate aging regulator, *nhr-28*, encodes a nuclear hormone receptor expressed in the pharynx, hypodermis, and intestine (Reece-Hoyes et al. 2007). NHR-28 ChIP-seq experiments performed on L4 larvae identified binding sites associated with 297 target genes that change expression with age (1.9-fold enriched, $p = 5.6 \times 10^{-36}$). The fosmid containing GFP-

tagged NHR-28 also contains *ace-1* (encoding a class A acetylcholinesterase) and *sur-7* (encoding a cation diffusion facilitator protein). The read density of sequences across the *nhr-28* gene region indicates that there are ~15 integrated copies of the fosmid in the modENCODE strain.

The second new candidate aging regulator is *nhr-76*, which encodes a nuclear hormone receptor expressed in body wall muscles, intestine, the excretory gland cell, pharynx, seam cells, and vulval muscles (Miyabayashi et al. 1999). The fosmid containing *nhr-76* also contains the majority of the K11H12.9 transcript (which encodes a protein kinase of unknown function), and is present at 3 or 4 copies in the modENCODE strain. Using the Naïve Bayes-derived method that selects the top 500 NHR-76 peaks, the NHR-76 ChIP-seq dataset was the second-most significantly enriched for age-regulated genes out of all of the modENCODE datasets (2.4-fold enriched, $p = 1.3 \times 10^{-15}$). However, using the first method that analyzed only the 50 significant low-complexity targets from the NHR-76 ChIP-seq experiment, only 12 were found to show altered expression with age (3.3-fold enriched, $p = 0.00017$). Thus, NHR-76 is an example where analysis using the Naïve Bayes-derived method is more sensitive in revealing candidate regulators.

A resource for identifying regulators of changes in *C. elegans* expression profiling experiments

There are currently over 1,000 *C. elegans* expression profiling experiments listed in the GEO database showing transcriptional changes at various developmental stages, different growth conditions and in different mutant backgrounds. For each of these, the ChIP-seq screening approach described above could be used to identify candidate causal regulators responsible for the observed expression changes. We have created a website through which users can perform a candidate regulator screen for any expression profiling experiment of interest (*http://celegansrwas.stanford.edu*).

Discussion

In *C. elegans*, the modENCODE consortium has provided a compendium of 98 ChIP-seq datasets for 57 transcription factors. In this work, we provide further evidence that integrating information across these ChIP-seq datasets can be highly informative for driving biological insights. By analyzing these datasets, we found that the number of transcription factors bound to a single DNA region (termed its complexity score) can vary widely, from one to fifty-four. Low-complexity binding sites are enriched for characterize factor-responsive expression, can be used to uncover mechanisms leading to regulation of distinct genes by a transcription factor between developmental stages and in different tissues, and can be screened to find novel transcriptional regulators of genes identified in expression profiling experiments. Each of these three analyses is enabled by the availability of a large number of ChIP-seq datasets.

In addition, we re-defined 296 Highly Occupied Target (HOT) regions that are bound by 38 or more factors (>65%). These HOT regions were associated with various types of housekeeping genes (including ribosomal proteins, *sl-2* splice leader transcripts, and *snoRNA*s), in agreement with the previous observation of HOT regions as associated with essential genes that are broadly and highly expressed (Gerstein et al. 2010).

Low-complexity targets correlate better with factor-responsive expression

The subset of transcription factor binding targets that are factor-responsive (i.e., activated or repressed by the factor in gain-of-function or loss-of-function experiments) can be used to infer functions and tissue-specificities of the transcription factor itself, as they represent targets for which expression will respond to altered regulator activity. However, the fraction of genes that are bound by a transcription factor and that are also responsive to changes in expression of the factor can range from 4% to over 50% (Spitz and Furlong 2012).

Previous work has shown that prediction of factor-responsive targets from an individual ChIP-seq experiment can be improved by incorporating additional information, such as co-correlated expression across hundreds of different microarray studies (Lai et al. 2010; Cheng et al. 2011; Marbach et al. 2012). Here, we show that by integrating 98 ChIP-seq datasets for 57 transcription factors, we can identify low-complexity binding sites that significantly improve the fraction of factor-responsive targets. In one instance (SKN-1 targets in L1 larvae), enrichment for activation by SKN-1 was only observed for the low-complexity sites. These results illustrate

insights using the aggregated results from the entire ChIP-seq compendium that are not possible using ChIP-seq data for just one transcription factor. Further, if the properties of transcription factor binding in humans are similar to *C. elegans*, our results suggest that incorporating binding site complexity for each bound region will improve analysis of transcription factor function in humans.

In this work we used a cutoff of eight or less transcription factors bound, based on analysis of HLH-1, to define low-complexity targets. Importantly, this criterion effectively segregated SKN-1 targets, indicating that the definition of low complexity targets works for other transcription factors as well. However, depending on the desired application, alternative complexity cutoffs could be chosen that shift the balance towards either greater sensitivity or specificity in identifying factor-responsive targets.

Mechanisms for tissue-specific regulation of downstream targets by UNC-62

Analyses of ChIP-seq experiments across multiple cell-types can reveal binding sites unique to individual cell types, which can be further studied to reveal insight into causal mechanisms. For example, analysis of MYC binding in two human cell-types revealed that GATA1 and TAL1 motifs correlated with MYC binding in K562 cells, whereas motifs for TEAD1 and the AP-1 complex correlated with binding specific to HeLaS3 cells (Shao et al. 2012). We observed that in *C. elegans*, UNC-62 showed dramatically different tissue-specificities among targets when assayed in different developmental stages. *unc-62* is alternatively spliced to produce two transcripts that include either exon 7a or 7b. Using ChIP-seq data, we observe that UNC-62 generally binds to one set of targets in the L2 or L3 larval stages and to a distinct set in adults. Our results suggest a model for tissue-specificity of UNC-62 binding in which UNC-62(7b) binds along with known co-factor HOX gene LIN-39 at one set of genes during early larval development, and UNC-62(7a) binds to a different set of genes in the intestine at an altered consensus motif without LIN-39 co-occupancy in adults.

Although we focused on UNC-62 as a proof-of-concept, the transcription factors SKN-1, PHA-4, and FOS-1 also showed enrichment for different tissues among their targets in different developmental stages. In addition, as many of the 57 transcription factors were only profiled in one stage, it is likely that more transcription factors will be found to bind to different targets at different points during development. Alternative isoforms that affect DNA binding domains and

combinatorial binding with co-factors are common mechanisms by which transcription factors regulate distinct sets of targets in different contexts (Taneri et al. 2004; Spitz and Furlong 2012). Thus, the type of analysis described here could provide insights into how other regulators achieve regulation of distinct sets of genes at different times and in different cell-types.

Screening ChIP-seq datasets for candidate transcription factors responsible for expression differences observed in expression profiling experiments

DNA microarray and high-throughput RNA sequencing technologies are commonly used to generate a list of genes that change expression in a mutant or altered growth condition. For such experiments, one often would like to identify the critical upstream regulators driving these changes in expression. One can gain insight into potential upstream regulators by searching for high levels of overlap between genes with altered expression and DNA regions bound by each transcription factor from a compendium of ChIP-seq experiments (Lachmann et al. 2010; Zambelli et al. 2012). These candidate upstream regulators can be further studied to confirm their role in regulating the genes that comprise the expression profile of interest. We validated this approach for HLH-1 and SKN-1 gene regulatory circuits, observing that this approach was successful for SKN-1 targets in L1 larvae only when low-complexity binding sites were used.

However, we note that several factors can limit the success of this approach. First, many transcription factors have not yet been profiled in ChIP-seq experiments by modENCODE. Second, some have different sets of targets in different tissues or at different times of development. For these factors, the conditions used for the ChIP-seq experiment needs to be matched to the conditions used for the expression profiling experiment. Finally, in some cases changes in the activity of an initial factor will initiate a cascade of changes in downstream regulators. In this case, expression profiling of worms mutant for the first factor will reveal the entire set of genes involved in the transcriptional cascade, including not only the primary targets of the first factor but also genes that are indirectly regulated. This cascade will hinder one's ability to identify the initial manipulation.

We observed a significant overlap between SKN-1 targets in the L1 stage and SKN-1-responsive genes in adults under oxidative stress, which could be larger if datasets matched for the same stage were used. However, it is infeasible to obtain ChIP-seq data for all factors in a large number of stages or conditions. Thus, our results with SKN-1 shows that upstream

regulators can be identified even when the ChIP-seq and expression profiling experiments are performed using different conditions.

Genomics screen for aging regulators

Next, we applied this method to the identification of new candidate regulators of aging in *C. elegans*. A variety of techniques have been utilized to identify specific regulators that are responsible for causing changes in expression in old age. For instance, a motif-driven approach was used to identify modules whose presence correlated with genes that changed expression with age (Adler et al. 2007). This led to the identification of the binding site for the transcription factor complex NF-KB as enriched in nine of ten tissues queried, suggesting that NF-KB is a candidate master regulator of aging in multiple tissues. NF-KB binding activity increases with age in various tissues and chemical inhibition of NF-KB activity led to a rejuvenation of aging phenotypes in the epidermis, suggesting that NF-KB is an important regulator of gene expression as well as detrimental phenotypes in old age (Adler et al. 2007).

In *C. elegans*, Budovskaya *et al.* (Budovskaya et al. 2008) found that GATA sequence motifs were enriched upstream of age-regulated genes, and identified GATA transcription factor ELT-3 as one of the factors responsible for expression changes between young and old worms. Expression of *elt-3* decreases with age, but worms that retain high levels of expression of *elt-3* in old age (due to knockdown of upstream repressors *elt-5* or *elt-6*) have increased lifespan, suggesting that ELT-3 may also be an important regulator of aging.

In this study, we compared genes altered during aging with genes bound by transcription factors in ChIP-seq datasets generated by the modENCODE consortium, identifying nine transcription factors with enriched binding to age-regulated genes. Two (ELT-3 and UNC-62) have previously been shown both to be directly responsible for changes in expression of downstream targets in old age as well as to modulate lifespan (Curran and Ruvkun 2007; Budovskaya et al. 2008; Van Nostrand et al. 2013). A third (SKN-1) is linked to aging through its role as an oxidative stress protective factor with decreased activity with age, and over-expression of constitutively active SKN-1 increases lifespan (Tullet et al. 2008; Przybysz et al. 2009). In addition to these three, we found that strains containing fosmids for two transcription factors (nuclear hormone receptors NHR-28 and NHR-76) had significantly extended lifespan.

Although they did not affect lifespan in simple knockdown or over-expression experiments, two of the remaining transcription factors (PQM-1 and FOS-1) may play a role in aging through their involvement in pathogen response, as pathogenicity significantly limits lifespan in *C. elegans* (Garigan et al. 2002; Shapira et al. 2006; Kao et al. 2011; Sanchez-Blanco and Kim 2011). Recent work has also implicated FOS-1 in modulation of lifespan by dietary restriction (Uno et al. 2013).

In summary, experimental evidence for as many as seven of the nine candidate regulators supports a role in the worm aging process. Further work will be required to determine whether the candidate transcription factors identified in this ChIP-seq screen are directly responsible for changes in expression of their downstream targets seen in the normal aging process. Although in this work we explore the model system of aging, the ChIP-seq screening approach described here could be used to help untangle complex regulatory networks responsible for expression changes in other expression profiles by identifying a small number of transcription factor candidates for further experimental study.

Methods

ChIP-seq datasets and analysis

98 ChIP-seq datasets for 57 transcription factors were obtained from the modENCODE consortium *http://submit.modencode.org/submit/public/list* or *http://data.modencode.org/*). Binding data were mapped to WS220 coordinates using scripts available from WormBase (*ftp://ftp.sanger.ac.uk/pub2/wormbase/software/Remap-between-versions/*) (Harris et al. 2010). Binding sites were then associated with annotated WS220 transcripts if the position of maximum read density within the binding site was: 1) located within the minimum of 5kb upstream of the annotated transcription start site or the distance to the nearest annotated protein coding gene, or 2) contained within the gene body (up to the annotated transcription stop site).

Using all 98 ChIP-seq datasets, the transcription factor complexity of every nucleotide in the genome was defined as the number of transcription factors that were found to have a significant binding site (q-value $\leq 10^{-5}$) that overlaps that region. The complexity of a binding site was defined as the maximum complexity of any position within the binding site. Overlapping binding sites for the same transcription factor observed in multiple developmental

stages were only counted once. For downstream analyses, genes with multiple binding sites of low-complexity and intermediate/high-complexity were counted for both groups.

Highly Occupied Target (HOT) regions were defined as contiguous genomic regions bound by at least 65% of the transcription factors considered (38 out of 57). Low-complexity binding sites were defined as those that had no position within the binding site that was enriched in 9 or more transcription factors (out of the 57 total). To associate HOT regions with nearby genes, a shorter 1kb upstream to 500nt downstream of transcription start site window was used, and the HOT region center was defined as the midpoint of the sub-region bound by the maximum number of factors within the HOT region. For enrichment analysis, 19 snRNA SL2 splice leader transcripts (*sls-2.#*), 76 small and large ribosomal subunit genes (*rps-#* and *rpl-#*), and 139 snoRNA transcripts were obtained from WormBase release WS220 (Harris et al. 2010). Gene Ontology annotations were obtained from Gene Ontology (Ashburner et al. 2000). Collagen genes were defined as genes annotated with NCBI KOG3544 (type IV and type XIII collagens).

Statistics and computational tools used

The degree of overlap between a ChIP-seq dataset and the various gene lists was calculated using the Matthews correlation coefficient, which provides a summary statistic that includes all four outcomes (true positives, true negatives, false positives, and false negatives) (Baldi et al. 2000). Significance of overlap was determined by Fisher's Exact test on the 2x2 contingency table (using the R statistics program), approximated with Yates' Chi-square test for datasets with expected and observed overlaps greater than 5. *P*-values for Chi-square tests were obtained using the *Perl* Statistics::Distributions module. For all analyses, enrichment was determined relative to the set of genes that were both present in the microarray or RNA-seq study and those in the WormBase WS220 release considered for ChIP-seq targets.

To calculate the percent of overlapping binding sites between ChIP-seq datasets, low-complexity binding sites for a first ChIP-seq dataset "A" were compared against all binding sites in a second ChIP-seq dataset ("B"). A binding site in the first dataset was considered to overlap with a binding site in the second if at least half of the smaller of the two binding sites was contained within the larger binding site. To avoid penalizing for the different number of binding sites identified across experiments, this procedure was repeated to compare low-complexity

binding sites in ChIP-seq dataset B against all binding sites in ChIP-seq dataset A), and the higher of the two percentages was used as the overlap between the two ChIP-seq datasets. To identify sequence motifs in UNC-62 binding sites, the 100 bp window surrounding the position of maximum ChIP-seq read density in each UNC-62 binding site was identified as the core binding region. 200 bp windows on either side of this core region served as the negative control. A *de novo* motif search was performed using the *Peak-Motifs* program (Thomas-Chollier et al. 2012), with the setting for 7-mer oligonucleotide length. Motif logos were generated using WebLogo (Crooks et al. 2004).

Gene expression datasets used

For HLH-1, 2128 genes that were significantly induced upon over-expression of HLH-1 in early embryos were obtained (Fukushige et al. 2006; Fox et al. 2007). For SKN-1, four microarrays of oxidative stress (GSM237006-GSM237009) as well as three microarrays of oxidative stress and *skn-1* RNAi (GSM237010-GSM237012) were used to identify SKN-1-responsive genes (Park et al. 2009). DNA microarray intensity values were scaled up or down to a target mean intensity value of 500, using only the central 96% of probes (2^{nd} to 98^{th} percentile). Probes that were not detected in all four control or all three *skn-1* RNAi microarrays were discarded, and an unpaired two-sample t-test was then used to identify genes with significantly altered expression upon *skn-1* RNAi. Using a cutoff of p-value ≤ 0.01 and requiring a 2-fold decrease in expression led to the identification of 91 SKN-1-responsive (activated) genes (Park et al. 2009). For analysis of UNC-62-responsive targets, 115 genes with significantly decreased expression and 67 genes with significantly increased expression upon knockdown of *unc-62* were obtained from GEO (GSE39574) (Van Nostrand et al. 2013)). To perform the screen for candidate regulators of aging, a dataset describing genes with significantly altered (both increased and decreased) expression with age was obtained (Budovskaya et al. 2008).

Tissue-enriched gene lists

Datasets of tissue-enriched and tissue-specific genes were obtained from previous publications as follows: tissue-enriched datasets for 25 tissues and tissue sub-types in various developmental stages (Spencer et al. 2011), intestine in L4 larvae (Pauli et al. 2006), muscle in L1 larvae (Roy et al. 2002), neurons and A-class neurons in embryos and L2 larvae (Von Stetina

et al. 2007), embryonic touch neurons (Zhang et al. 2002), embryonic motor neurons (Fox et al. 2005), and embryonic AFD and AWD neurons (Colosimo et al. 2004). Annotations of known transcription factor expression profiles were obtained from WormBase (Harris et al. 2010).

Naïve Bayes responsiveness score

The scoring metric that combines *q*-value and complexity was created using a simple two-feature Naïve Bayes classification model. For each ChIP-seq binding site, the discrete *q*-values were segmented into bins (where a bin from x to y indicates binding sites with x ≤ *q*-value < y): 10^{-2} to $5x10^{-3}$, $5x10^{-3}$ to 10^{-4}, 10^{-4} to 10^{-5}, 10^{-5} to $10^{-7.5}$, $10^{-7.5}$ to 10^{-10}, 10^{-10} to 10^{-15}, 10^{-15} to 10^{-25}, and 10^{-25} to 0. Complexity was similarly binned, based upon whether the binding site was bound (in total) by 1, 2, 3-4, 5-6, 7-9, 10-12, 13-15, 16-20, 21-25, 26-31, 32-37, or 38-57 transcription factors.

To initially test the method, Naïve Bayes classifiers were independently trained upon each ChIP-seq dataset to compare training error for predicting HLH-1-responsive genes across ChIP-seq datasets. After training, for a binding site with *q*-value $\hat{q}$ and complexity $\hat{r}$ the classifier yields a probability of that binding site being associated with the HLH-1 responsive (y=1) or non-responsive (y=0) class. The log of the ratio of these probabilities ($\frac{p(y=1|\hat{q},\hat{r})}{p(y=0|\hat{q},\hat{r})}$) was used as a score for each binding site; the top scoring 500 binding sites for each factor were used to determine the predictive ability of each ChIP-seq dataset on HLH-1-responsive genes.

For further analyses, the classifier was trained using HLH-1 ChIP-seq targets and HLH-1 factor-responsive genes, and then used to score binding sites from the other 97 ChIP-seq datasets. In all downstream analyses, the 500 binding sites with the highest log ratio score were used.

Lifespan analysis

General *C. elegans* techniques as well as lifespan experiments were performed as previously described (Budovskaya et al. 2008). Unless otherwise noted, lifespan experiments were performed by placing day 1 adult worms (with visible eggs) on NGM plates containing 30 uM 5-fluoro-2'-deoxyuridine (FUDR). Deaths before day 7 of adulthood were censured. Log-rank tests were performed using OASIS (Yang et al. 2011). RNAi clones used were obtained from the Ahringer RNAi library (Kamath et al. 2003) and sequenced to verify proper insertions.

RNAi knockdown experiments in adults were performed on NGM plates supplemented with 30 uM FUDR, 100 ug/mL Ampicillin, and 2 mM IPTG to induce dsRNA expression.

For over-expression, strains were obtained from modENCODE in which a fosmid containing a transcription factor (with a C-terminal GFP fusion) is over-expressed along with an *unc-119* transgene as a selectable marker in an *unc-119(ed3)* background. As controls, we used four strains (RW11108, RW11206, RW10780, and RW10384) that also contain a biolistically bombarded and integrated *unc-119* transgene. These strains lack over-expression of a transcription factor, but instead contain a promoter fusion to a histone-tagged mCherry fluorescent reporter (and showed weak or no expression of mCherry). For the initial screen of all nine transcription factors, the modENCODE strain used for the ChIP-seq experiments was used without backcrossing; strains containing NHR-28 (OP317) or NHR-76 (OP203) fosmids that showed significant extension of lifespan in the initial screen were then backcrossed twice to wild-type (N2) and repeated to confirm extension of lifespan. Strain OP203 had a tendency to move onto the walls of the plate, increasing the number of worms lost in the experiment; for the backcrossed lifespan experiment, a ring of palmitic acid (10 mg/mL) was added around the plate in an attempt to alleviate this concern.

To estimate fosmid insertion copy number, read density in the ChIP-seq input control samples was used in a manner similar to previously described (Sarov et al. 2012). The average read density across sliding 10kb windows was calculated for the entire genome, and copy number was defined as the ratio between the average read density in windows within the fosmid and the average of all other windows in the genome.

Acknowledgements

We thank the modENCODE consortium for providing ChIP-seq data. Some strains were provided by the CGC, which is funded by NIH Office of Research Infrastructure Programs (P40 OD010440). We thank Anne Brunet, Arend Sidow, Michael Snyder, and members of the Kim lab for helpful discussion, suggestions and improvements. We thank members of the Kim lab and Jeanine Frey for critical reading of the manuscript. E.V.N. has been supported by the Stanford Genome Training Program and the Smith Fellowship (Stanford Graduate Fellowships program). Research in the laboratory of S.K.K. is supported by the NHGRI, NIGMS, NIA and the Glenn Foundation.

Figure Legends

Figure 1. Examples of highly occupied and low-complexity regions of transcription factor binding. Binding of 57 transcription factors in one or more developmental stages (98 ChIP-seq datasets in total) were obtained from the *C. elegans* modENCODE consortium and are shown for two examples. Datasets are shown in identical order to Supplemental Table 1. (A) Binding proximal to translation elongation factor 1-alpha homolog *eef-1A.1*. A ~450 nt HOT region indicated by the red dashed box is significantly enriched for binding in ChIP-seq analyses of 44 different transcription factors. Transcription factor complexity (the number of factors with ChIP-seq binding sites overlapping that position) is shown at the top. Below, regions of significant enrichment (q-value $\leq 10^{-5}$) observed in each of the 98 ChIP-seq datasets are shown as black boxes. (B) Low-complexity HLH-1 binding proximal to HLH-1-activated target *pat-3* is shown.

Figure 2. Highly Occupied Target (HOT) regions. (A) The histogram indicates the number of genomic regions observed for different binding complexities. In blue, thousands of low-complexity regions are bound by 8 or fewer factors; in red, 296 HOT regions are bound by 38 or more transcription factors. (B) HOT regions tend to be located close to the transcription start sites (TSS) of genes. The cumulative distribution plot shows the cumulative fraction of regions (y-axis) that have a maximal distance to the nearest annotated transcription start site indicated on the x-axis. HOT regions have significantly shorter distances to nearby transcription start sites than low-complexity regions ($p = 1.7\text{x}10^{-23}$; Kolmogorov-Smirnov test). Results shown here are for all annotated genes (WS220); similar results were observed using only protein-coding genes (data not shown).

Figure 3. Low Binding site complexity correlates with factor-responsive expression. (A) Using 4191 significant HLH-1 binding sites identified by the modENCODE consortium (Niu et al. 2011), the set of genes with HLH-1 binding sites with complexity less than or equal to n (for n = 1 to 57) were identified. Each set was then compared to 2128 genes activated upon HLH-1 over-expression (Fukushige et al. 2006; Fox et al. 2007), with the percent of directly bound targets activated indicated in red. Except for complexities of 2 or less, binding sites with lower complexity had higher precision in predicting HLH-1-activated genes. Using the Matthews correlation coefficient (in blue) to weight both false-positives and false-negatives, a complexity of 8 or less was identified as optimal for predicting factor-responsive targets (indicated by *). (B) Using only binding sites with complexity of 8 or less significantly improves prediction of HLH-1-responsive binding. Circles indicate the set of genes with any HLH-1 binding site (top), or only those with low-complexity or intermediate/high-complexity binding sites (bottom). The overlap with HLH-1-activated genes is indicated in red, with the expected overlap indicated by white hash marks. Significance of enrichment was calculated by Yates' chi-square test. (C-D) The same complexity criteria significantly delineate SKN-1 targets in L2 and L1 larvae. Circles indicate 91 SKN-1-activated genes (Park et al. 2009), with the percent overlap with SKN-1 ChIP-seq datasets indicated in blue and expected overlap indicated by white hash marks. (C) Low-complexity regions for SKN-1 in L2 larvae (C), and L1 larvae (D) are enriched for genes responsive to *skn-1* knockdown. Enrichment significance was determined by Fisher's Exact test.

The set of all SKN-1 targets in L1 was not significantly enriched for SKN-1-activated genes (1.1-fold-enriched, $p > 0.5$), indicating that the correlation between SKN-1 binding in L1 larvae and SKN-1-responsive expression is only observed when binding site complexity is taken into account.

Figure 4. Distinct sets of targets bound by UNC-62 in L2/L3 larvae and adults. (A) Strains expressing isoform-specific *unc-62* translational reporters show stage- and tissue-specific expression (Van Nostrand et al. 2013). (left) *unc-62(7a):GFP* is not observed in early larval stages, but is highly expressed in the intestine in late larval stages and young adults (YA). (right) *unc-62(7b):GFP* is not observed in the intestine at any stage, but is expressed in the hypodermis (hyp), the ventral nerve cord (vnc), and other neurons (neu). Strains were imaged in a *glo-4(ok623)* background to limit gut autofluorescence. (B) The overlap of ChIP-seq binding sites for UNC-62 in L2 and L3 larvae, young adults (YA), and HOX transcription factor LIN-39 in L3 are shown as the percent of binding sites in the smaller set that are also bound in the larger. (C) Targets bound by UNC-62 in L2, L3, and YA, as well as those bound by LIN-39 in L3 larvae, were compared to genes enriched for expression in various tissues (Roy et al. 2002; Zhang et al. 2002; Colosimo et al. 2004; Fox et al. 2005; Pauli et al. 2006; Von Stetina et al. 2007; Spencer et al. 2011). Colors indicate the correlation between low-complexity target genes and genes with tissue-enriched expression for the indicated tissue. Tissues are clustered according to broad tissue types, and the specific tissue for each column is listed in Supplemental Fig. 2 and Supplemental Table 3. Int, intestine; Hyp, hypodermis; BWM, body wall muscle. (D) A *de novo* motif search with RSAT (Thomas-Chollier et al. 2012) identifies sequences significantly enriched in the 100 bp central core region of UNC-62 binding sites. 200 bp flanking regions on either side of this core were used as the background sequence set. Both motifs contain the *D. melonogaster* Homothorax motif (TGACA) (Noyes et al. 2008).

Figure 5. Identifying candidate regulators of expression profiling datasets. To predict candidate regulators of genes altered in expression profiling experiments, low-complexity targets from each of the 98 ChIP-seq datasets were compared against (A) 2128 genes activated by *hlh-1* (Fukushige et al. 2006; Fox et al. 2007), (B) 91 genes activated by *skn-1* (Park et al. 2009), or (C) 115 genes decreased upon knockdown of *unc-62* (Van Nostrand et al. 2013). For each ChIP-seq dataset (*y*-axis), the *x*-axis indicates the overlap between low-complexity targets and genes altered in the transcriptome profiling experiment, with enrichment indicated by positive values and depletion by negative values. (A) HLH-1 low-complexity ChIP-seq targets in mixed embryos (MxE) showed the greatest enrichment for *hlh-1*-activated genes (* indicates $p < 10^{-100}$, $\chi^2 = 1047$ by Yates' chi-squared test). (B) SKN-1 targets in L2 larvae ($p = 6.3 \times 10^{-22}$), followed by SKN-1 targets in L1 larvae ($p = 7.5 \times 10^{-7}$) showed the greatest enrichment for *skn-1*-activated genes. (C) UNC-62 targets did not correlate with *unc-62*-activated genes, potentially indicating that most genes with decreased expression upon *unc-62* knockdown are secondary targets of UNC-62. (D) To control for the different number of targets between ChIP-seq datasets, we developed a score (based on a Naïve-Bayes classifier) for each binding site that reflects both the binding site significance (*q*-value) as well as binding site complexity. This classifier was trained on the set of HLH-1 ChIP-seq targets and *hlh-1*-activated genes, and the 500 binding sites for each ChIP-seq dataset with the highest scores were then tested on *skn-1*-activated genes. Using this method, SKN-1 targets showed the greatest correlation (3.6-fold enriched, $p = 7.9 \times 10^{-9}$ in L1 larvae and 5.1-fold enriched, $p = 9.8 \times 10^{-9}$ in L2 larvae) for *skn-1*-activated genes.

Figure 6. Identification of candidate regulators of aging. (A-B) The ChIP-seq-based screening approach described in Fig. 5 was applied to the set of genes with altered expression during aging (Budovskaya et al. 2008). For each ChIP-seq dataset, the correlation was calculated twice: first (A), using all low-complexity binding sites, and second (B), using the 500 binding sites with the highest Naïve Bayes-derived score as described in Fig. 5D. Bars indicate the *p*-value ($\log_{10}$) between age-regulated genes and the indicated ChIP-seq targets, with enrichment indicated by positive values and depletion indicated by negative values. For nine transcription factors, significant overlap ($p < 10^{-5}$) was observed using at least one of the two approaches; six of nine were significant with both. Black checkmarks indicate three factors (ELT-3, UNC-62, and SKN-1) for which modulation has been shown to increase lifespan (Curran and Ruvkun 2007; Budovskaya et al. 2008; Tullet et al. 2008). Red checkmarks indicate factors for which the modENCODE strain (which contains an integrated multi-copy fosmid containing the listed transcription factor) has an extended lifespan. (C-D) Lifespan of modENCODE-generated strains in which a strain containing a fosmid with C-terminal GFP-tagged *nhr-28* or *nhr-76* was compared to controls. Days of adulthood are indicated on the *x*-axis, and percent of worms remaining alive is indicated on the *y*-axis. (C) Strain OP371 (containing a fosmid with GFP-tagged *nhr-28*) was compared to three controls (RW10780, RW11206, and RW11175). The strain over-expressing *nhr-28* shows 15-30% extension of lifespan relative to the various controls (all $p < 10^{-5}$ by log-rank test). (D) Strain OP203 (containing a fosmid with GFP-tagged *nhr-76*) showed a 7-15% increase in mean lifespan relative to two controls (RW10780 and RW11206)($p < 0.01$ against either). Lifespan data shown is from strains that were backcrossed twice to wild-type; each lifespan experiment was performed twice before backcrossing and gave similar results (Supplemental Table 5).

Supplemental Figure 1. Low-complexity binding sites correlate with factor-responsive expression. (A) Additional metrics for comparison of HLH-1 ChIP-seq targets with HLH-1 factor-responsive genes. The set of genes with HLH-1 binding sites with complexity less than or equal to *n* (for $n = 1$ to 57) were each queried for their ability to predict HLH-1-responsive genes. Red indicates positive predictive value, green indicates sensitivity, blue indicates specificity, and teal indicates the Matthews correlation. (B) SKN-1 ChIP-seq targets were compared to SKN-1-responsive genes in a similar matter to HLH-1 in (A) and Figure 3A. Orange indicates SKN-1 ChIP-seq targets in L1 larvae, and red indicates targets in L2 larvae. (C) Gene complexity does not improve the correlation with factor responsiveness compared to binding site complexity. To test whether the total number of transcription factors bound to a gene could explain the observed correlation between binding site complexity and factor-responsive expression, the analysis in Fig. 3A was repeated using a gene complexity score (defined as the number of transcription factors bound anywhere within the gene body or promoter region). Regardless of the complexity threshold, the correlation between HLH-1 binding and *hlh-1*-responsive expression using gene-based complexity (black) was always below the maximal correlation observed with binding site-based complexity (blue).

Supplemental Figure 2. Tissue-enriched expression of transcription factor targets. Low-complexity targets from each of 98 ChIP-seq datasets were compared against genes with tissue-enriched expression datasets (Roy et al. 2002; Zhang et al. 2002; Colosimo et al. 2004; Fox et al. 2005; Pauli et al. 2006; Von Stetina et al. 2007; Spencer et al. 2011), as listed in Supplemental

Table 3. Blue indicates datasets with negative Matthews correlation for a tissue-enriched gene set, whereas red indicates enriched targets. Transcription factors were hierarchically clustered along the *y*-axis; tissues (on the *x*-axis) were manually grouped into five tissue-types: Int, intestine; Hyp, hypodermis; BWM, body wall muscle, and others (not labeled).

Supplemental Figure 3. Concordance between tissue-enriched target expression and annotated TF expression. 13 transcription factors showed high correlation (> 0.2) with one or more tissue-enriched gene sets for neurons and neuronal subtypes (N), hypodermis (H), intestine (I), or body wall muscle (M), described in Supplemental Fig. 2. For these 13, the expression pattern of the transcription factor itself was obtained from Wormbase (Harris et al. 2010). 12 of the 13 factors were expressed in the tissue in which the targets were enriched (green), whereas only one was not expressed in the predicted tissue (red). Additionally, many factors showed expression in either entire tissues (blue) or specific tissue sub-types (light blue) in which the targets were not enriched.

Supplemental Figure 4. UNC-62 is not highly expressed in the intestine in the L3 stage ChIP-seq experiment. The modENCODE UNC-62 L3 ChIP-seq experiment was performed on strain OP600 that contains an integrated *unc-62:GFP* transgene. Representative images indicate that *unc-62:GFP* is not yet highly expressed in the intestine in the OP600 L3 worms isolated and prepared for ChIP-seq 36 hrs after feeding from a starved population of L1 stage worms.

Supplemental Figure 5. Comparisons of *hlh-1*-, *skn-1*-, and *unc-62*-responsive genes with ChIP-seq datasets. As in Fig. 5, targets from each of the 98 ChIP-seq datasets were compared against (A-B) 2128 genes activated by HLH-1 (Fukushige et al. 2006; Fox et al. 2007), (C) 91 genes activated by SKN-1 (Park et al. 2009), (D) 115 genes decreased upon knockdown of *unc-62* (Van Nostrand et al. 2013), and (E) 67 genes increased upon knockdown of *unc-62* (Van Nostrand et al. 2013). ChIP-seq datasets are listed along the *y*-axis, with the significance of overlap from a Fisher's Exact test (or Yates' Chi-square test where appropriate) indicated on the *x*-axis. Enrichment is indicated by positive values and depletion by negative values. Unless otherwise noted, significant (*q-value* < 10^{-5}) low-complexity targets are used. (A) A Naïve Bayes classifier was trained independently on each ChIP-seq dataset for prediction of HLH-1-activated genes, and the training error of the 500 top scoring binding sites for each were then compared to HLH-1-activated genes. HLH-1 targets were most significantly enriched (* indicates $p < 10^{-100}$, $\chi^2 = 761$ by Yates' chi-squared test), with five additional factors enriched at a $p < 10^{-30}$ cutoff. (B) One classifier was trained on HLH-1 ChIP-seq targets and HLH-1-activated genes, and then used to score binding sites in all other 97 ChIP-seq datasets. HLH-1 targets were again the most significantly enriched (* indicates $p < 10^{-100}$, $\chi^2 = 761$ by Yates' chi-squared test), with three additional factors enriched at a $p < 10^{-30}$ cutoff. (C) SKN-1-activated genes were compared against all binding sites (regardless of complexity) for each ChIP-seq dataset. Only SKN-1 targets in L2 larvae were significantly enriched (1.9-fold enriched, $p = 2.7 \times 10^{-7}$). Note that whereas SKN-1 targets in L1 larvae was the second-most significantly enriched for SKN-1-activated genes when low-complexity targets are used (Fig. 5B), the SKN-1 (L1) dataset is missed when all targets are used. (D) Analysis of the 67 genes repressed by UNC-62 in young adults does not reveal UNC-62, indicating that most UNC-62-repressed genes are likely secondary targets. (E) Analysis of UNC-62-activated genes in young adults using the top 500

binding sites, instead of low-complexity binding sites (as in Fig. 5C) does not improve the correlation between UNC-62 ChIP-seq targets and UNC-62-activated genes.

Supplemental Table 1. Number of binding sites for each ChIP-seq dataset.

ChIP-seq dataset	All[a]	Significant[b]	Significant and low complexity[c]
AHA-1 (L1)	473	123	3
AHA-1 (L4)	1449	343	20
ALR-1 (L2)	6081	2398	1076
ALY-2 (L1)	5520	2522	1081
ALY-2 (L2)	2862	351	133
ALY-2 (L3)	4186	1500	741
BLMP-1 (L1)	10072	7382	4511
C01B12.2 (L2)	9222	5096	1425
C16A3.4 (L1)	3228	1525	16
CEH-14 (L2)	5144	1265	339
CEH-16 (L2)	1846	676	209
CEH-26 (LE)	4633	1030	113
CEH-30 (LE)	5859	1958	255
CES-1 (L1)	2723	856	380
CES-1 (L3)	2579	542	229
CES-1 (L4)	2791	501	214
DAF-12 (L3)	1043	166	8
DPL-1 (L1)	4951	2607	309
DPL-1 (L4)	9610	4438	822
DPY-27 (MxE)	425	132	14
EGL-27 (L1)	3434	745	14
EGL-27 (L2)	8551	3120	549
EGL-27 (L3)	1845	364	7
EGL-5 (L3)	4631	1213	476
ELT-3 (L1)	5292	2731	967
ELT-3 (L3)	1495	242	39
EOR-1 (L3)	14520	11187	8706
EOR-1 (L3b)	6791	3258	278
F16B12.6 (L1)	1601	965	164
F45C12.2 (L1)	4636	2512	190
F45C12.2 (L2)	1486	372	3
F45C12.2 (L3)	2074	704	37
FKH-2 (L3)	2980	207	19
FOS-1 (L1)	5854	2405	201
FOS-1 (L2)	8595	5452	2422
FOS-1 (L3)	5379	1445	269
FOS-1 (L4)	3055	698	124
GEI-11 (L2)	4304	1594	318

GEI-11 (L3)	5990	2531	452
GEI-11 (L4)	683	222	101
GEI-11 (YA)	2732	747	281
HAM-1 (L1)	5607	3072	396
HLH-1 (MxE)	12437	4702	2136
LIN-11 (L2)	2329	738	48
LIN-13 (MxE)	5367	1897	315
LIN-15B (L1)	2319	915	15
LIN-15B (L3)	4120	2378	198
LIN-15B (L4)	995	292	3
LIN-39 (L3)	7345	3014	1191
LIR-2 (L3)	1719	196	18
MAB-5 (L3)	4400	1465	297
MDL-1 (L1)	9240	4823	819
MEF-2 (L1)	970	246	5
MEP-1 (MxE)	10688	5233	1746
MML-1 (L3)	382	114	12
NHR-11 (L2)	2186	568	53
NHR-116 (L2)	1359	211	118
NHR-129 (L2)	10594	7628	3997
NHR-28 (L3)	1740	272	43
NHR-28 (L4)	9354	6019	3004
NHR-6 (L2)	7682	3904	1690
NHR-76 (L3)	2660	471	59
NHR-77 (L1)	5776	2430	363
NHR-77 (L2)	3128	519	29
NHR-77 (L3)	5821	1278	265
NHR-77 (L4)	11725	5952	2292
PEB-1 (L2)	1577	331	90
PES-1 (L4)	6995	3000	661
PHA-4 (L1)	8637	6311	3192
PHA-4 (L2)	7543	3997	1438
PHA-4 (L4)	3890	1069	278
PHA-4 (LE)	8980	5202	1953
PHA-4 (MxE)	8704	4347	1426
PHA-4 (stL1)	7359	4803	2802
PHA-4 (YA)	2416	697	134
PQM-1 (L3)	5782	3196	1594
R02D3.7 (L2)	2928	876	105
R02D3.7 (L3)	7493	3846	718
R02D3.7 (L4)	2362	788	199

SEA-2 (L3)	1297	216	4
SEM-4 (L2)	7362	2820	661
SKN-1 (L1)	7302	3137	513
SKN-1 (L2)	9194	3044	970
SMA-9 (L2)	826	139	10
UNC-130 (L1)	2634	539	99
UNC-62 (L1)	1107	132	7
UNC-62 (L2)	2227	426	47
UNC-62 (L3)	4077	1193	231
UNC-62 (YA)	4358	1272	339
W03F9.2 (YA)	12065	5892	2128
ZAG-1 (L1)	2068	319	18
ZAG-1 (L2)	4001	1516	285
ZAG-1 (L3)	2214	577	22
ZAG-1 (L4)	4207	955	146
ZK377.2 (L1)	2249	295	17
ZK377.2 (L2)	4575	1827	133
ZK377.2 (L3)	2491	776	21
ZK377.2 (L4)	8088	4249	1006

[a] All binding sites identified by modENCODE (with q-value ≤ 0.01)
[b] Significant binding sites with q-value $\leq 10^{-5}$
[c] Significant and low-complexity sites with q-value $\leq 10^{-5}$ and complexity ≤ 8

Supplemental Table 2. Gene Ontology analysis of HOT regions.

GO category	GO description	# of HOT-associated genes in GO class[a]	Fold-enrichment	p-value (log_{10})[b]
GO:0000003	reproduction	98	6.00	-86.61
GO:0002119	nematode larval development	86	5.65	-69.98
GO:0009792	embryo development ending in birth or egg hatching	111	4.55	-68.70
GO:0040007	growth	68	5.34	-50.74
GO:0040010	positive regulation of growth rate	63	4.19	-33.41
GO:0005622	intracellular	37	5.89	-30.80
GO:0006898	receptor-mediated endocytosis	32	5.71	-25.53
GO:0040035	hermaphrodite genitalia development	35	5.30	-25.39
GO:0040011	locomotion	50	4.07	-25.22
GO:0005840	ribosome	20	20.33	-15.66
GO:0003735	structural constituent of ribosome	20	19.72	-15.66
GO:0006412	translation	21	13.21	-15.64
GO:0010171	body morphogenesis	24	4.10	-12.04
GO:0008340	determination of adult lifespan	23	3.54	-9.21
GO:0018996	molting cycle, collagen and cuticulin-based cuticle	15	5.60	-6.69
GO:0005524	ATP binding	23	2.91	-6.58
GO:0040027	negative regulation of vulval development	12	6.89	-6.34
GO:0018991	oviposition	14	5.41	-6.11

GO:0005737	cytoplasm	13	5.54	-5.82
GO:0040018	positive regulation of multicellular organism growth	14	4.56	-5.29
GO:0003746	translation elongation factor activity	4	52.86	-5.24
GO:0015935	small ribosomal subunit	4	52.86	-5.24

[a] Genes were associated with HOT regions if the HOT region was within 1kb upstream or downstream of the annotated transcription start site

[b] Significance of overlap was determined by Fisher's Exact test, or approximated by Yates' chi-square test where appropriate (see Methods)

Supplemental Table 3. Tissue-enriched gene sets used.

Tissue	Reference	method	# of genes
AFD and AWD neurons (emb)	Colosimo, M.E., *et al.* (2004)	FACS sorted cells[a]	563
motor neurons (emb)	Fox, R.M., *et al.* (2005)	FACS sorted cells	810
A-class neurons (emb)	Von Stetina, S.E., *et al.* (2007)	FACS sorted cells	895
pan-neuronal (emb)	Von Stetina, S.E., *et al.* (2007)	FACS sorted cells	1491
A-class neurons (L2)	Von Stetina, S.E., *et al.* (2007)	mRNA-tagging[b]	373
pan-neuronal (L2)	Von Stetina, S.E., *et al.* (2007)	mRNA-tagging	1383
touch neurons (emb)	Zhang, Y., *et al.* (2002)	FACS sorted cells	61
BAG neurons (EE)	Spencer, W.C., *et al.* (2011)	FACS sorted cells	454
A-class neurons (L2)	Spencer, W.C., *et al.* (2011)	mRNA-tagging	692
GABA neurons (L2)	Spencer, W.C., *et al.* (2011)	mRNA-tagging	132
glr-1+ neurons (L2)	Spencer, W.C., *et al.* (2011)	mRNA-tagging	662
pan-neuronal (L2)	Spencer, W.C., *et al.* (2011)	mRNA-tagging	1012
dopaminergic neurons (L3-L4)	Spencer, W.C., *et al.* (2011)	mRNA-tagging	1232
PVD/OLL neurons (L3-L4)	Spencer, W.C., *et al.* (2011)	mRNA-tagging	878
A-class neurons (LE)	Spencer, W.C., *et al.* (2011)	FACS sorted cells	393
AVA neurons (LE)	Spencer, W.C., *et al.* (2011)	FACS sorted cells	540
AVE neurons (LE)	Spencer, W.C., *et al.* (2011)	FACS sorted cells	433
dopaminergic neurons (LE)	Spencer, W.C., *et al.* (2011)	FACS sorted cells	474
GABA neurons (LE)	Spencer, W.C., *et al.* (2011)	FACS sorted cells	364
pan-neuronal (LE)	Spencer, W.C., *et al.* (2011)	FACS sorted cells	459
germline precursors (EE)	Spencer, W.C., *et al.* (2011)	FACS sorted cells	974
excretory cell (L2)	Spencer, W.C., *et al.* (2011)	mRNA-tagging	528
coelomocytes (L2)	Spencer, W.C., *et al.* (2011)	mRNA-tagging	228
coelomocytes (LE)	Spencer, W.C., *et al.* (2011)	FACS sorted cells	576
pharyngeal muscle (LE)	Spencer, W.C., *et al.* (2011)	FACS sorted cells	598
CEPsh (YA)	Spencer, W.C., *et al.* (2011)	mRNA-tagging	296
bodywall muscle (L2)	Spencer, W.C., *et al.* (2011)	mRNA-tagging	1148
bodywall muscle (LE)	Spencer, W.C., *et al.* (2011)	FACS sorted cells	397
non-pharyngeal muscle (L1)	Roy, P., *et al.* (2002)	mRNA-tagging	1127
hypodermis (LE)	Spencer, W.C., *et al.* (2011)	FACS sorted cells	739
hypodermis (L3-L4)	Spencer, W.C., *et al.* (2011)	mRNA-tagging	1248
intestine (L2)	Spencer, W.C., *et al.* (2011)	mRNA-tagging	945
intestine (LE)	Spencer, W.C., *et al.* (2011)	FACS sorted cells	887
intestine (L4)	Pauli, F., *et al.* (2006)	mRNA-tagging	1597

[a] The FACS sorting method to identify embryonic cells expressing a tissue-specific promoter is described in Zhang, Y., *et al.* (2002) (Zhang et al. 2002)
[b] The mRNA-tagging method to preferentially pull down mRNAs expressed in a desired tissue is described in Roy, P., *et al.* (2002) (Roy et al. 2002)

Supplemental Table 4. Lifespan effect of RNAi treatment of putative aging regulatory transcription factors.

Strain	RNAi	N	Mean lifespan	Standard error	% lifespan extension	*p*-value[a]
N2	*empty vector*	134	19.12	0.32	-	-
N2	*fos-1*	122	17.97	0.36	-6.0	0.024
N2	*C01B12.2*	67	19.4	0.53	1.5	0.15
N2	*nhr-77*	66	19.64	0.47	2.7	0.25
N2	*empty vector*	267	20.55	0.3	-	-
N2	*skn-1*	135	18.22	0.24	-11.3	$< 10^{-8}$
N2	*C01B12.2*	112	20.82	0.49	1.3	0.33
N2	*nhr-28*	123	20.16	0.38	-1.9	0.18
N2	*nhr-77*	128	22.03	0.45	7.2	0.0036
N2	*unc-62*	55	24.36	0.88	18.5	5.5×10^{-8}
N2	*empty vector*	75	15.03	0.51	-	-
N2	*pqm-1*	64	14.31	0.43	-4.8	0.0916
N2	*elt-3*	39	17.05	0.9	13.4	0.0266
N2	*nhr-76*	54	13.74	0.36	-8.6	0.0325

[a] *p*-values were calculated in Oasis (Yang et al. 2011) using the log-rank test.

Supplemental Table 5. Lifespan of strains over-expressing putative aging regulatory transcription factors.

Strain	Transcription Factor	N	Mean lifespan	Standard error	% lifespan extension[a]	*p*-value[a]
SD1876 (OP317 2x b.c.[b])	*nhr-28*	103	23.9	0.67	18.3	$< 10^{-5}$
SD1886 (RW11108 2x b.c.[b])	-[c]	62	17.81	0.74		
SD1896 (RW11206 2x b.c.[b])	-	120	20.2	0.51		
SD1895 (RW10780 2x b.c.[b])	-	103	18.9	0.43		
SD1891 (OP203 2x b.c.[b])[d]	*nhr-76*	102	22.2	0.86	6.7	0.0014
SD1895 (RW10780 2x b.c.[b])[d]	-	121	20.8	0.5		
SD1896 (RW11206 2x b.c.[b])[d]	-	129	19.2	0.55		
OP317	*nhr-28*	138	22.3	0.44	8.3	$< 10^{-5}$
OP304	*fos-1*	111	17.3	0.4	-17.3	
OP343	*C01B12.2*	121	16.2	0.41	-21.5	
OP178	*skn-1*	128	20.1	0.58	-2.3	
RW10384	-	53	20.6	0.63		
RW11206	-	126	18.5	0.41		
OP353	*nhr-77*	141	14.4	0.35	-26.6	
OP317	*nhr-28*	134	22.8	0.34	16.7	$< 10^{-5}$
OP203	*nhr-76*	64	22.9	1.31	17.2	$< 10^{-5}$
RW11108	-	139	14.8	0.32		
RW11206	-	141	19.5	0.33		
RW10780	-	142	17.3	0.42		
RW10384	-	142	17.1	0.5		
OP203	*nhr-76*	32	21.8	1.55	13.0	0.0004
OP600	*unc-62*	63	20.4	0.94	5.9	0.0259
OP75	*elt-3*	74	18.0	0.55	-6.5	
OP201	*pqm-1*	79	17.4	0.66	-9.9	
RW10384	-	85	19.3	0.47		
RW11108	-	98	18.1	0.54		

RW11206	-	85	18.3	0.48

[a] *p*-values were calculated in Oasis (Yang et al. 2011) using the log-rank test. Lifespan extensions as well as *p*-values shown are compared to the longest-living control strain assayed in the same experiment.
[b] Indicated strains were controls backcrossed twice to wild-type (N2) as follows: SD1876 (backcrossed OP317), SD1886 (backcrossed RW11108), SD1896 (backcrossed RW11026), and SD1895 (backcrossed RW10780).
[c] Controls were *unc-119(ed3)* worms containing a low-copy integrated rescue of wild-type *unc-119*, as well as a promoter fusion to histone protein-tagged mCherry (and thus do not over-express a transcription factor). Controls were further selected as strains in which mCherry expression was dim or absent.
[d] Palmitic acid (10 mg/mL) was added in a ring around the edge of the plates to prevent worms from leaving the plate, as *nhr-76* over-expression appears to cause a social behavior defect.

References

Adler AS, Sinha S, Kawahara TL, Zhang JY, Segal E, Chang HY. 2007. Motif module map reveals enforcement of aging by continual NF-kappaB activity. *Genes Dev* **21**(24): 3244-3257.

An JH, Blackwell TK. 2003. SKN-1 links C. elegans mesendodermal specification to a conserved oxidative stress response. *Genes Dev* **17**(15): 1882-1893.

Ashburner M, Ball CA, Blake JA, Botstein D, Butler H, Cherry JM, Davis AP, Dolinski K, Dwight SS, Eppig JT et al. 2000. Gene ontology: tool for the unification of biology. The Gene Ontology Consortium. *Nat Genet* **25**(1): 25-29.

Baldi P, Brunak S, Chauvin Y, Andersen CA, Nielsen H. 2000. Assessing the accuracy of prediction algorithms for classification: an overview. *Bioinformatics* **16**(5): 412-424.

Biggin MD. 2011. Animal transcription networks as highly connected, quantitative continua. *Dev Cell* **21**(4): 611-626.

Bowerman B, Eaton BA, Priess JR. 1992. skn-1, a maternally expressed gene required to specify the fate of ventral blastomeres in the early C. elegans embryo. *Cell* **68**(6): 1061-1075.

Budovskaya YV, Wu K, Southworth LK, Jiang M, Tedesco P, Johnson TE, Kim SK. 2008. An elt-3/elt-5/elt-6 GATA transcription circuit guides aging in C. elegans. *Cell* **134**(2): 291-303.

Cheng C, Alexander R, Min R, Leng J, Yip KY, Rozowsky J, Yan KK, Dong X, Djebali S, Ruan Y et al. 2012. Understanding transcriptional regulation by integrative analysis of transcription factor binding data. *Genome Res* **22**(9): 1658-1667.

Cheng C, Yan KK, Yip KY, Rozowsky J, Alexander R, Shou C, Gerstein M. 2011. A statistical framework for modeling gene expression using chromatin features and application to modENCODE datasets. *Genome Biol* **12**(2): R15.

Colosimo ME, Brown A, Mukhopadhyay S, Gabel C, Lanjuin AE, Samuel AD, Sengupta P. 2004. Identification of thermosensory and olfactory neuron-specific genes via expression profiling of single neuron types. *Curr Biol* **14**(24): 2245-2251.

Crooks GE, Hon G, Chandonia JM, Brenner SE. 2004. WebLogo: a sequence logo generator. *Genome Res* **14**(6): 1188-1190.

Curran SP, Ruvkun G. 2007. Lifespan regulation by evolutionarily conserved genes essential for viability. *PLoS Genet* **3**(4): e56.

Fox RM, Von Stetina SE, Barlow SJ, Shaffer C, Olszewski KL, Moore JH, Dupuy D, Vidal M, Miller DM, 3rd. 2005. A gene expression fingerprint of C. elegans embryonic motor neurons. *BMC Genomics* **6**: 42.

Fox RM, Watson JD, Von Stetina SE, McDermott J, Brodigan TM, Fukushige T, Krause M, Miller DM, 3rd. 2007. The embryonic muscle transcriptome of Caenorhabditis elegans. *Genome Biol* **8**(9): R188.

Fukushige T, Brodigan TM, Schriefer LA, Waterston RH, Krause M. 2006. Defining the transcriptional redundancy of early bodywall muscle development in C. elegans: evidence for a unified theory of animal muscle development. *Genes Dev* **20**(24): 3395-3406.

Fukushige T, Krause M. 2005. The myogenic potency of HLH-1 reveals wide-spread developmental plasticity in early C. elegans embryos. *Development* **132**(8): 1795-1805.

Gao F, Foat BC, Bussemaker HJ. 2004. Defining transcriptional networks through integrative modeling of mRNA expression and transcription factor binding data. *BMC Bioinformatics* **5**: 31.

Garber M, Yosef N, Goren A, Raychowdhury R, Thielke A, Guttman M, Robinson J, Minie B, Chevrier N, Itzhaki Z et al. 2012. A High-Throughput Chromatin Immunoprecipitation Approach Reveals Principles of Dynamic Gene Regulation in Mammals. *Mol Cell*.

Garigan D, Hsu AL, Fraser AG, Kamath RS, Ahringer J, Kenyon C. 2002. Genetic analysis of tissue aging in Caenorhabditis elegans: a role for heat-shock factor and bacterial proliferation. *Genetics* **161**(3): 1101-1112.

Gerstein MB, Kundaje A, Hariharan M, Landt SG, Yan KK, Cheng C, Mu XJ, Khurana E, Rozowsky J, Alexander R et al. 2012. Architecture of the human regulatory network derived from ENCODE data. *Nature* **489**(7414): 91-100.

Gerstein MB Lu ZJ Van Nostrand EL Cheng C Arshinoff BI Liu T Yip KY Robilotto R Rechtsteiner A Ikegami K et al. 2010. Integrative analysis of the Caenorhabditis elegans genome by the modENCODE project. *Science* **330**(6012): 1775-1787.

Harris TW, Antoshechkin I, Bieri T, Blasiar D, Chan J, Chen WJ, De La Cruz N, Davis P, Duesbury M, Fang R et al. 2010. WormBase: a comprehensive resource for nematode research. *Nucleic Acids Res* **38**(Database issue): D463-467.

Jiang Y, Shi H, Liu J. 2009. Two Hox cofactors, the Meis/Hth homolog UNC-62 and the Pbx/Exd homolog CEH-20, function together during C. elegans postembryonic mesodermal development. *Dev Biol* **334**(2): 535-546.

Johnson DS, Mortazavi A, Myers RM, Wold B. 2007. Genome-wide mapping of in vivo protein-DNA interactions. *Science* **316**(5830): 1497-1502.

Kamath RS, Fraser AG, Dong Y, Poulin G, Durbin R, Gotta M, Kanapin A, Le Bot N, Moreno S, Sohrmann M et al. 2003. Systematic functional analysis of the Caenorhabditis elegans genome using RNAi. *Nature* **421**(6920): 231-237.

Kao CY, Los FC, Huffman DL, Wachi S, Kloft N, Husmann M, Karabrahimi V, Schwartz JL, Bellier A, Ha C et al. 2011. Global functional analyses of cellular responses to pore-forming toxins. *PLoS Pathog* **7**(3): e1001314.

Krivega I, Dean A. 2012. Enhancer and promoter interactions-long distance calls. *Curr Opin Genet Dev* **22**(2): 79-85.

Kuntz SG, Williams BA, Sternberg PW, Wold BJ. 2012. Transcription factor redundancy and tissue-specific regulation: Evidence from functional and physical network connectivity. *Genome Res* **22**(10): 1907-1919.

Kvon EZ, Stampfel G, Yanez-Cuna JO, Dickson BJ, Stark A. 2012. HOT regions function as patterned developmental enhancers and have a distinct cis-regulatory signature. *Genes Dev* **26**(9): 908-913.

Lachmann A, Xu H, Krishnan J, Berger SI, Mazloom AR, Ma'ayan A. 2010. ChEA: transcription factor regulation inferred from integrating genome-wide ChIP-X experiments. *Bioinformatics* **26**(19): 2438-2444.

Lai F, Chang JS, Wu WS. 2010. Identifying a Transcription Factor's Regulatory Targets from its Binding Targets. *Gene Regul Syst Bio* **4**: 125-133.

Lei H, Liu J, Fukushige T, Fire A, Krause M. 2009. Caudal-like PAL-1 directly activates the bodywall muscle module regulator hlh-1 in C. elegans to initiate the embryonic muscle gene regulatory network. *Development* **136**(8): 1241-1249.

Loh YH, Wu Q, Chew JL, Vega VB, Zhang W, Chen X, Bourque G, George J, Leong B, Liu J et al. 2006. The Oct4 and Nanog transcription network regulates pluripotency in mouse embryonic stem cells. *Nat Genet* **38**(4): 431-440.

MacArthur S, Li XY, Li J, Brown JB, Chu HC, Zeng L, Grondona BP, Hechmer A, Simirenko L, Keranen SV et al. 2009. Developmental roles of 21 Drosophila transcription factors are determined by quantitative differences in binding to an overlapping set of thousands of genomic regions. *Genome Biol* **10**(7): R80.

Maduro MF, Meneghini MD, Bowerman B, Broitman-Maduro G, Rothman JH. 2001. Restriction of mesendoderm to a single blastomere by the combined action of SKN-1 and a GSK-3beta homolog is mediated by MED-1 and -2 in C. elegans. *Mol Cell* **7**(3): 475-485.

Marbach D, Roy S, Ay F, Meyer PE, Candeias R, Kahveci T, Bristow CA, Kellis M. 2012. Predictive regulatory models in Drosophila melanogaster by integrative inference of transcriptional networks. *Genome Res* **22**(7): 1334-1349.

Miyabayashi T, Palfreyman MT, Sluder AE, Slack F, Sengupta P. 1999. Expression and function of members of a divergent nuclear receptor family in Caenorhabditis elegans. *Dev Biol* **215**(2): 314-331.

Moorman C, Sun LV, Wang J, de Wit E, Talhout W, Ward LD, Greil F, Lu XJ, White KP, Bussemaker HJ et al. 2006. Hotspots of transcription factor colocalization in the genome of Drosophila melanogaster. *Proc Natl Acad Sci U S A* **103**(32): 12027-12032.

Negre N, Brown CD, Ma L, Bristow CA, Miller SW, Wagner U, Kheradpour P, Eaton ML, Loriaux P, Sealfon R et al. 2011. A cis-regulatory map of the Drosophila genome. *Nature* **471**(7339): 527-531.

Niu W, Lu ZJ, Zhong M, Sarov M, Murray JI, Brdlik CM, Janette J, Chen C, Alves P, Preston E et al. 2011. Diverse transcription factor binding features revealed by genome-wide ChIP-seq in C. elegans. *Genome Res* **21**(2): 245-254.

Noyes MB, Christensen RG, Wakabayashi A, Stormo GD, Brodsky MH, Wolfe SA. 2008. Analysis of homeodomain specificities allows the family-wide prediction of preferred recognition sites. *Cell* **133**(7): 1277-1289.

Park SK, Tedesco PM, Johnson TE. 2009. Oxidative stress and longevity in Caenorhabditis elegans as mediated by SKN-1. *Aging Cell* **8**(3): 258-269.

Pauli F, Liu Y, Kim YA, Chen PJ, Kim SK. 2006. Chromosomal clustering and GATA transcriptional regulation of intestine-expressed genes in C. elegans. *Development* **133**(2): 287-295.

Potts MB, Wang DP, Cameron S. 2009. Trithorax, Hox, and TALE-class homeodomain proteins ensure cell survival through repression of the BH3-only gene egl-1. *Dev Biol* **329**(2): 374-385.

Przybysz AJ, Choe KP, Roberts LJ, Strange K. 2009. Increased age reduces DAF-16 and SKN-1 signaling and the hormetic response of Caenorhabditis elegans to the xenobiotic juglone. *Mech Ageing Dev* **130**(6): 357-369.

Reece-Hoyes JS, Shingles J, Dupuy D, Grove CA, Walhout AJ, Vidal M, Hope IA. 2007. Insight into transcription factor gene duplication from Caenorhabditis elegans Promoterome-driven expression patterns. *BMC Genomics* **8**: 27.

Ren B, Robert F, Wyrick JJ, Aparicio O, Jennings EG, Simon I, Zeitlinger J, Schreiber J, Hannett N, Kanin E et al. 2000. Genome-wide location and function of DNA binding proteins. *Science* **290**(5500): 2306-2309.

Roy PJ, Stuart JM, Lund J, Kim SK. 2002. Chromosomal clustering of muscle-expressed genes in Caenorhabditis elegans. *Nature* **418**(6901): 975-979.

Roy S, Ernst J, Kharchenko PV, Kheradpour P, Negre N, Eaton ML, Landolin JM, Bristow CA, Ma L, Lin MF et al. 2010. Identification of functional elements and regulatory circuits by Drosophila modENCODE. *Science* **330**(6012): 1787-1797.

Sanchez-Blanco A, Kim SK. 2011. Variable pathogenicity determines individual lifespan in Caenorhabditis elegans. *PLoS Genet* **7**(4): e1002047.

Sarov M, Murray JI, Schanze K, Pozniakovski A, Niu W, Angermann K, Hasse S, Rupprecht M, Vinis E, Tinney M et al. 2012. A genome-scale resource for in vivo tag-based protein function exploration in C. elegans. *Cell* **150**(4): 855-866.

Shao Z, Zhang Y, Yuan GC, Orkin SH, Waxman DJ. 2012. MAnorm: a robust model for quantitative comparison of ChIP-Seq data sets. *Genome Biol* **13**(3): R16.

Shapira M, Hamlin BJ, Rong J, Chen K, Ronen M, Tan MW. 2006. A conserved role for a GATA transcription factor in regulating epithelial innate immune responses. *Proc Natl Acad Sci U S A* **103**(38): 14086-14091.

Spencer WC, Zeller G, Watson JD, Henz SR, Watkins KL, McWhirter RD, Petersen S, Sreedharan VT, Widmer C, Jo J et al. 2011. A spatial and temporal map of C. elegans gene expression. *Genome Res* **21**(2): 325-341.

Spitz F, Furlong EE. 2012. Transcription factors: from enhancer binding to developmental control. *Nat Rev Genet* **13**(9): 613-626.

Taneri B, Snyder B, Novoradovsky A, Gaasterland T. 2004. Alternative splicing of mouse transcription factors affects their DNA-binding domain architecture and is tissue specific. *Genome Biol* **5**(10): R75.

Thomas-Chollier M, Herrmann C, Defrance M, Sand O, Thieffry D, van Helden J. 2012. RSAT peak-motifs: motif analysis in full-size ChIP-seq datasets. *Nucleic Acids Res* **40**(4): e31.

Tullet JM, Hertweck M, An JH, Baker J, Hwang JY, Liu S, Oliveira RP, Baumeister R, Blackwell TK. 2008. Direct inhibition of the longevity-promoting factor SKN-1 by insulin-like signaling in C. elegans. *Cell* **132**(6): 1025-1038.

Uno M, Honjoh S, Matsuda M, Hoshikawa H, Kishimoto S, Yamamoto T, Ebisuya M, Yamamoto T, Matsumoto K, Nishida E. 2013. A Fasting-Responsive Signaling Pathway that Extends Life Span in C. elegans. *Cell reports* **3**(1): 79-91.

Van Auken K, Weaver D, Robertson B, Sundaram M, Saldi T, Edgar L, Elling U, Lee M, Boese Q, Wood WB. 2002. Roles of the Homothorax/Meis/Prep homolog UNC-62 and the Exd/Pbx homologs CEH-20 and CEH-40 in C. elegans embryogenesis. *Development* **129**(22): 5255-5268.

Van Nostrand EL, Sánchez-Blanco A, Wu B, Nguyen A, Kim SK. 2013. Roles of the Developmental Regulator unc-62/Homothorax in Limiting Longevity in Caenorhabditis elegans. . *PLoS Genet* **9(2)**: e1003325.

Von Stetina SE, Watson JD, Fox RM, Olszewski KL, Spencer WC, Roy PJ, Miller DM, 3rd. 2007. Cell-specific microarray profiling experiments reveal a comprehensive picture of gene expression in the C. elegans nervous system. *Genome Biol* **8**(7): R135.

Wagmaister JA, Gleason JE, Eisenmann DM. 2006. Transcriptional upregulation of the C. elegans Hox gene lin-39 during vulval cell fate specification. *Mech Dev* **123**(2): 135-150.

Wang J, Zhuang J, Iyer S, Lin X, Whitfield TW, Greven MC, Pierce BG, Dong X, Kundaje A, Cheng Y et al. 2012. Sequence features and chromatin structure around the genomic regions bound by 119 human transcription factors. *Genome Res* **22**(9): 1798-1812.

Yang JS, Nam HJ, Seo M, Han SK, Choi Y, Nam HG, Lee SJ, Kim S. 2011. OASIS: online application for the survival analysis of lifespan assays performed in aging research. *PLoS One* **6**(8): e23525.

Yang L, Sym M, Kenyon C. 2005. The roles of two C. elegans HOX co-factor orthologs in cell migration and vulva development. *Development* **132**(6): 1413-1428.

Yip KY, Cheng C, Bhardwaj N, Brown JB, Leng J, Kundaje A, Rozowsky J, Birney E, Bickel P, Snyder M et al. 2012. Classification of human genomic regions based on experimentally determined binding sites of more than 100 transcription-related factors. *Genome Biol* **13**(9): R48.

Zambelli F, Prazzoli GM, Pesole G, Pavesi G. 2012. Cscan: finding common regulators of a set of genes by using a collection of genome-wide ChIP-seq datasets. *Nucleic Acids Res* **40**(Web Server issue): W510-515.

Zhang Y, Ma C, Delohery T, Nasipak B, Foat BC, Bounoutas A, Bussemaker HJ, Kim SK, Chalfie M. 2002. Identification of genes expressed in C. elegans touch receptor neurons. *Nature* **418**(6895): 331-335.

Zhong M, Niu W, Lu ZJ, Sarov M, Murray JI, Janette J, Raha D, Sheaffer KL, Lam HY, Preston E et al. 2010. Genome-wide identification of binding sites defines distinct functions for Caenorhabditis elegans PHA-4/FOXA in development and environmental response. *PLoS Genet* **6**(2): e1000848.

Figure 1

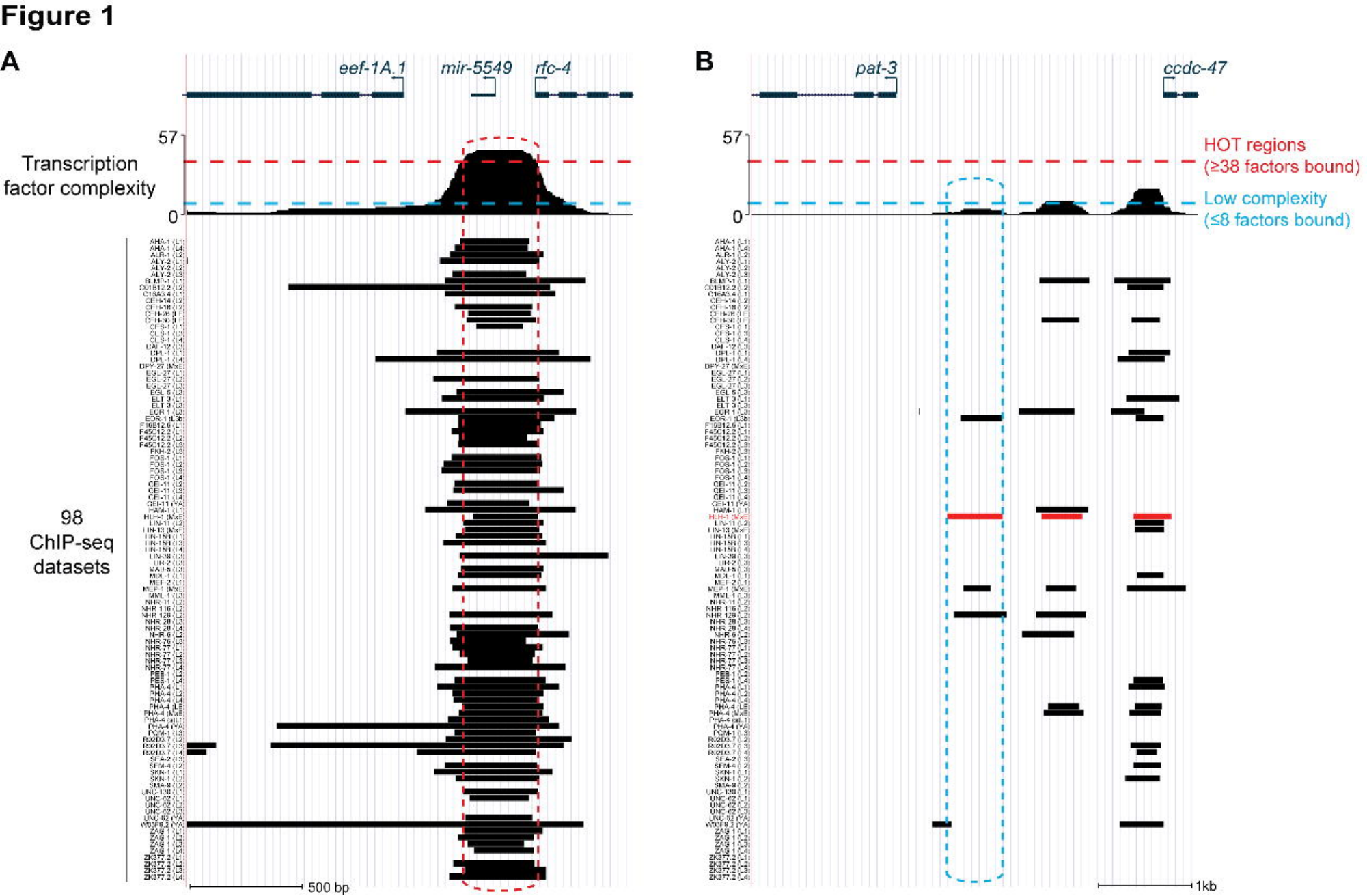
A
eef-1A.1
mir-5549
rfc-4
57
0
Transcription factor complexity
98 ChIP-seq datasets
500 bp
B
pat-3
ccdc-47
57
0
HOT regions (≥38 factors bound)
Low complexity (≤8 factors bound)
1kb

Figure 2

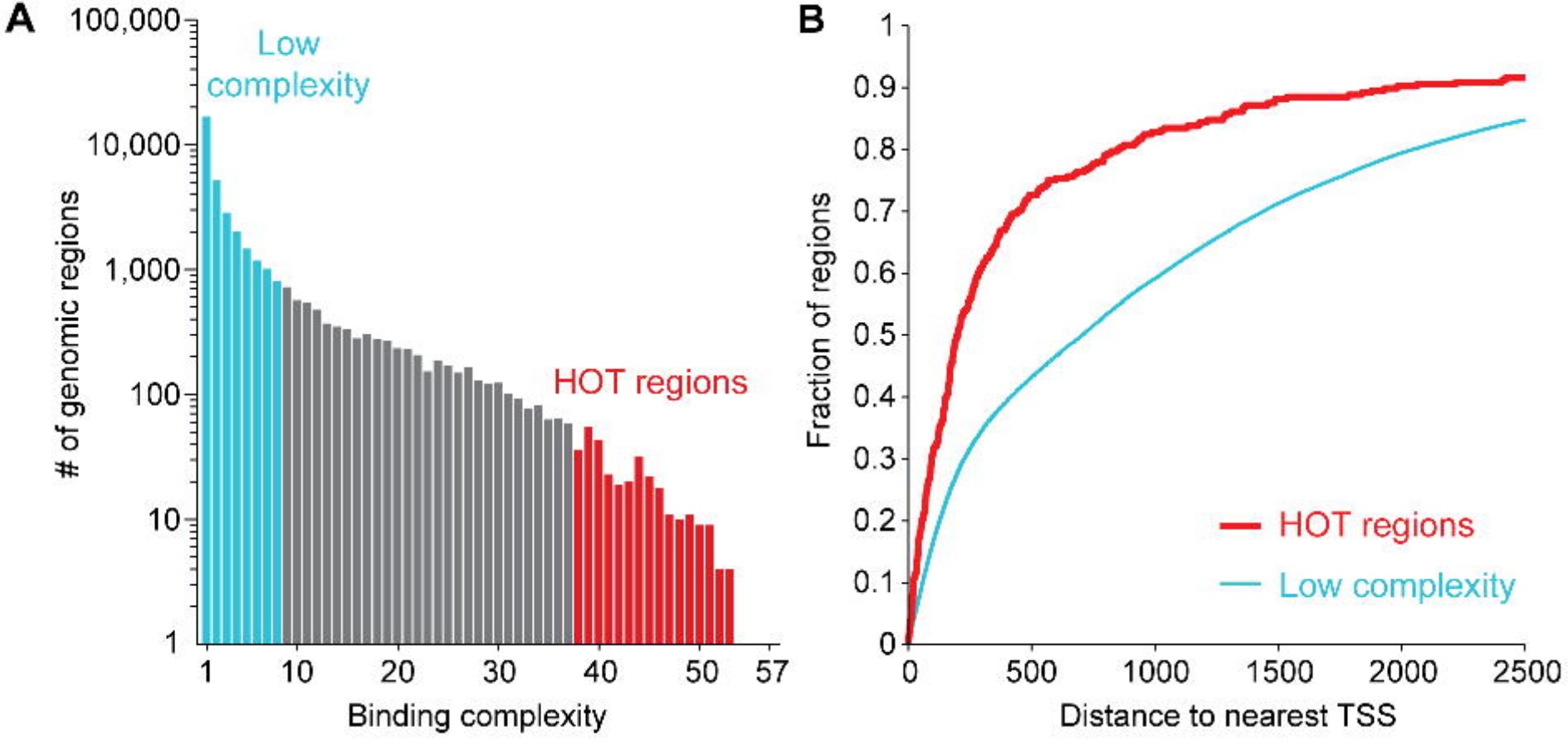
A
100,000
10,000
1,000
100
10
1
# of genomic regions
Low complexity
HOT regions
1
10
20
30
40
50
57
Binding complexity
B
1
0.9
0.8
0.7
0.6
0.5
0.4
0.3
0.2
0.1
0
Fraction of regions
HOT regions
Low complexity
0
500
1000
1500
2000
2500
Distance to nearest TSS

Figure 3

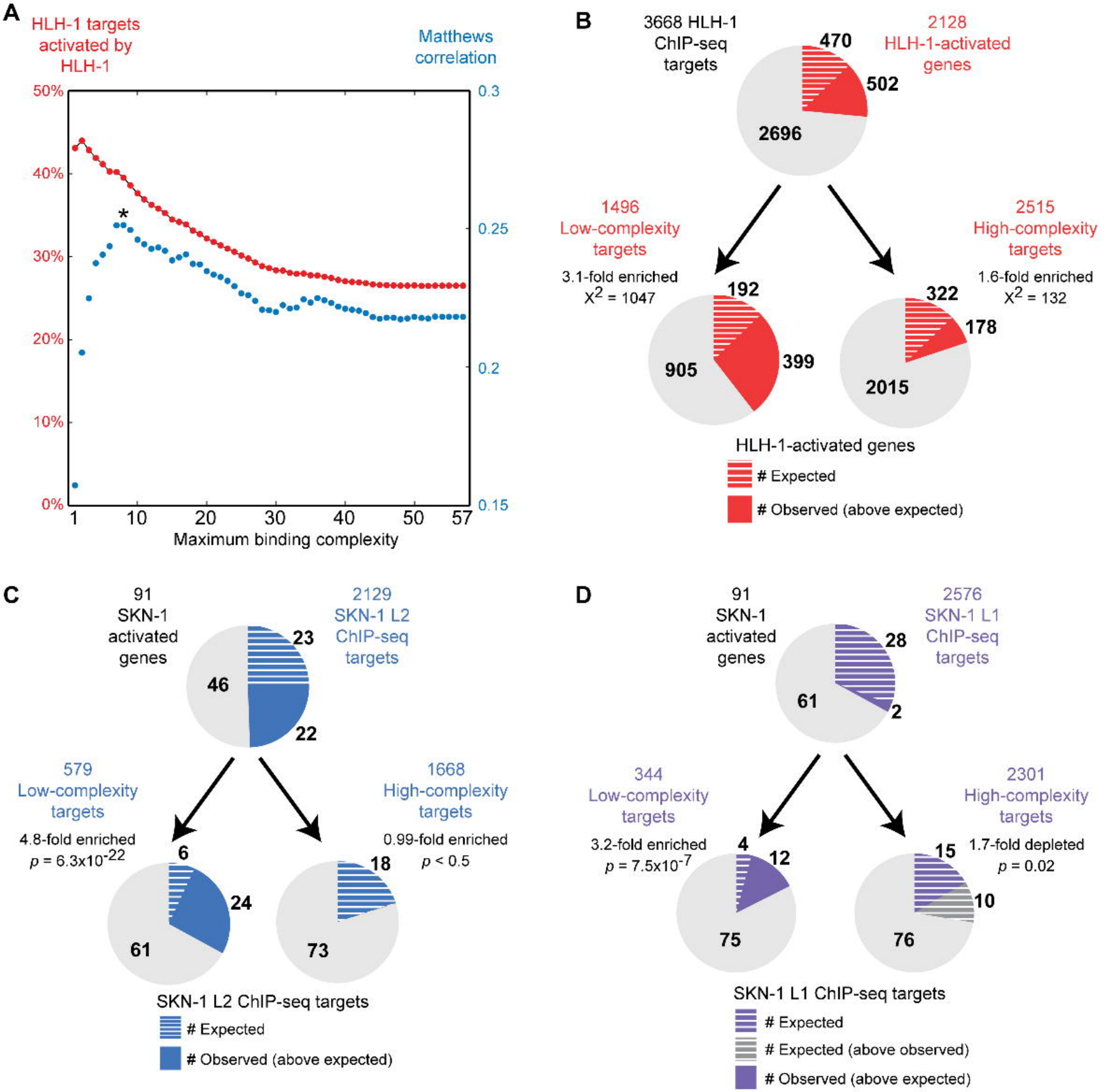
A
HLH-1 targets activated by HLH-1
Matthews correlation
50%
40%
30%
20%
10%
0%
0.3
0.25
0.2
0.15
1
10
20
30
40
50
57
Maximum binding complexity
*
B
3668 HLH-1 ChIP-seq targets
2128 HLH-1-activated genes
470
502
2696
1496 Low-complexity targets
3.1-fold enriched
X2 = 1047
192
399
905
2515 High-complexity targets
1.6-fold enriched
X2 = 132
322
178
2015
HLH-1-activated genes
Expected
Observed (above expected)
C
91 SKN-1 activated genes
2129 SKN-1 L2 ChIP-seq targets
23
46
22
579 Low-complexity targets
4.8-fold enriched
p = 6.3x10-22
6
24
61
1668 High-complexity targets
0.99-fold enriched
p < 0.5
18
73
SKN-1 L2 ChIP-seq targets
Expected
Observed (above expected)
D
91 SKN-1 activated genes
2576 SKN-1 L1 ChIP-seq targets
28
61
2
344 Low-complexity targets
3.2-fold enriched
p = 7.5x10-7
4
12
75
2301 High-complexity targets
1.7-fold depleted
p = 0.02
15
10
76
SKN-1 L1 ChIP-seq targets
Expected
Expected (above observed)
Observed (above expected)

Figure 4

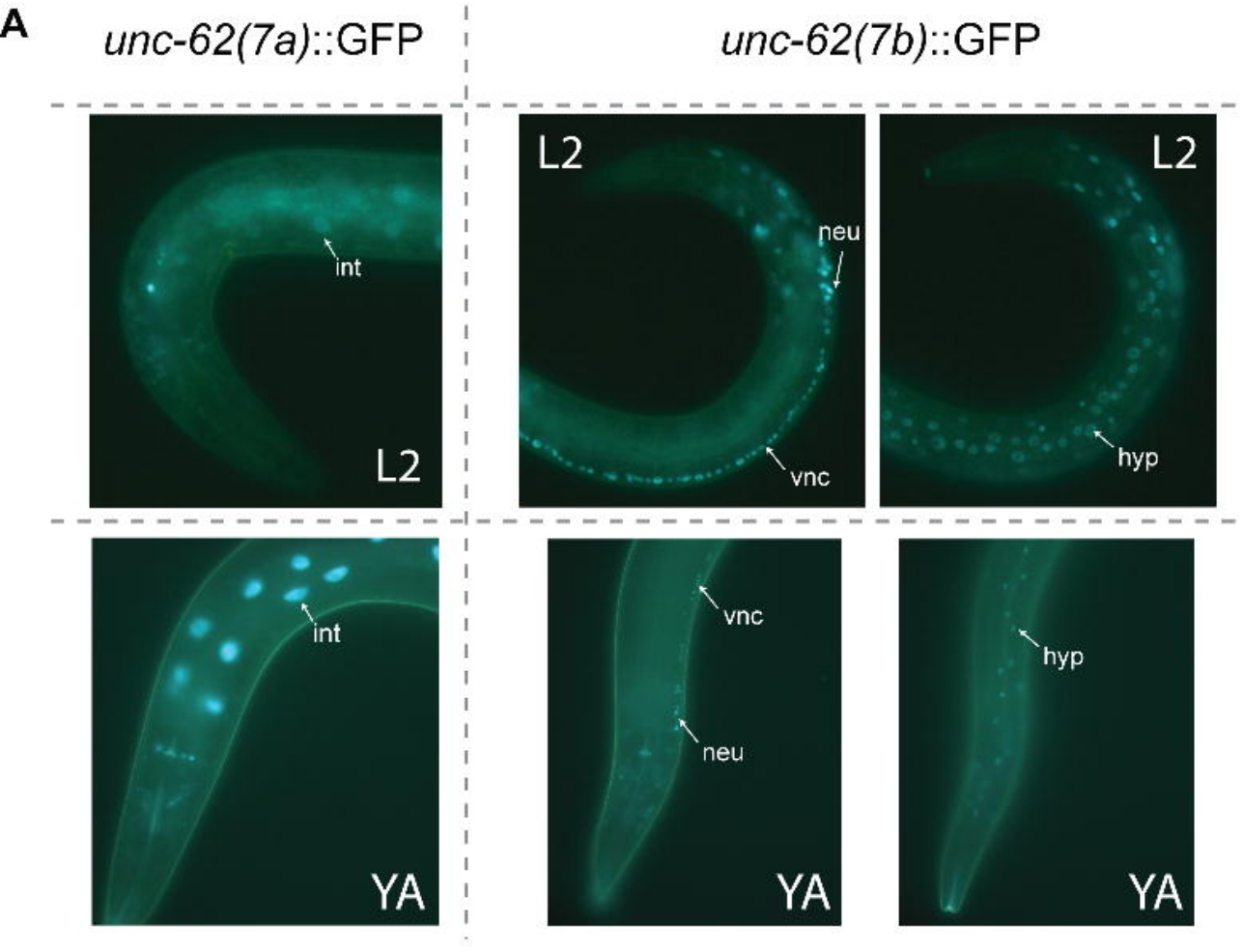
A
unc-62(7a)::GFP
unc-62(7b)::GFP
L2
int
L2
neu
vnc
L2
hyp
YA
int
YA
vnc
neu
YA
hyp

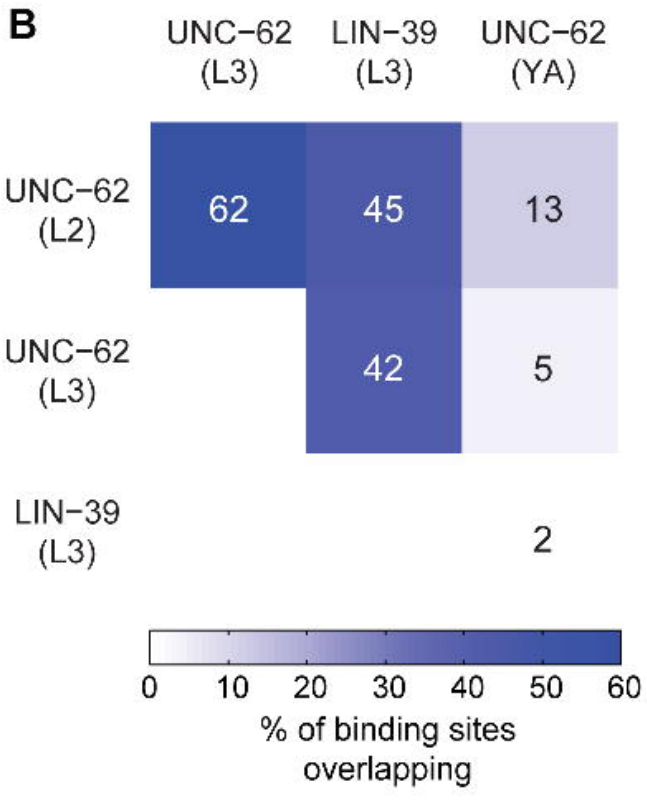
B
UNC−62 (L3)
LIN−39 (L3)
UNC−62 (YA)
UNC−62 (L2)
62
45
13
UNC−62 (L3)
42
5
LIN−39 (L3)
2
0
10
20
30
40
50
60
% of binding sites overlapping

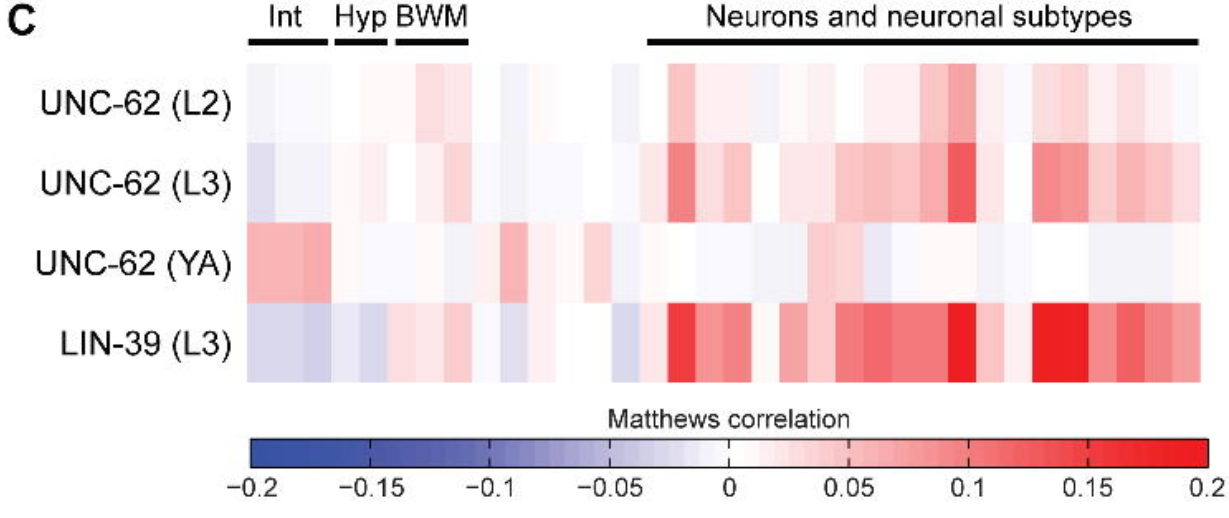
C
Int
Hyp
BWM
Neurons and neuronal subtypes
UNC-62 (L2)
UNC-62 (L3)
UNC-62 (YA)
LIN-39 (L3)
Matthews correlation
−0.2
−0.15
−0.1
−0.05
0
0.05
0.1
0.15
0.2

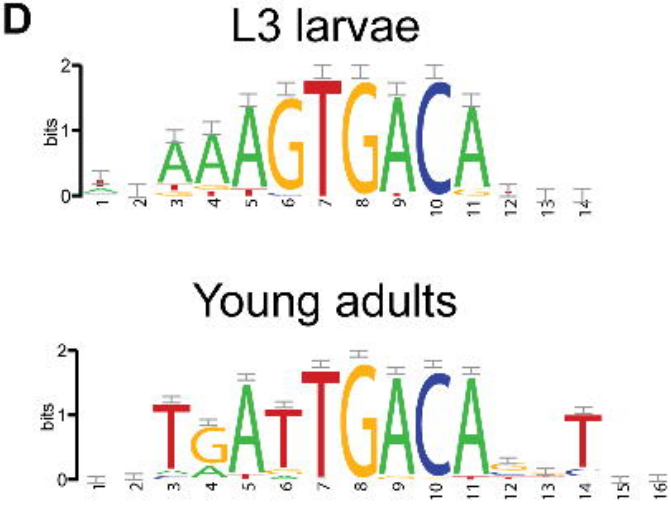
D
L3 larvae
bits
AAAGTGACA
Young adults
bits
TGATTGACA

Figure 5

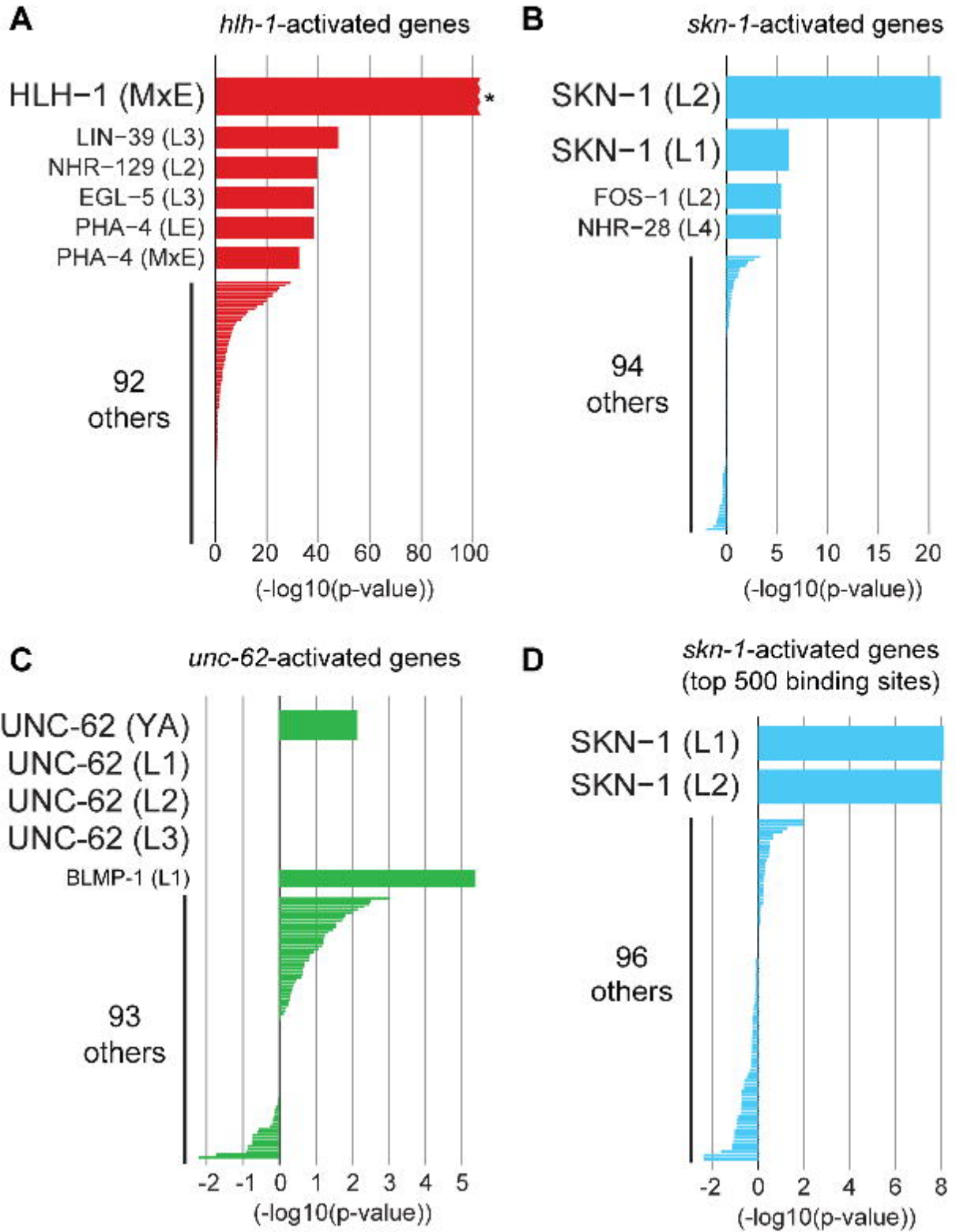
A
hlh-1-activated genes
HLH−1 (MxE)
*
LIN−39 (L3)
NHR−129 (L2)
EGL−5 (L3)
PHA−4 (LE)
PHA−4 (MxE)
92 others
0 20 40 60 80 100
(-log10(p-value))
B
skn-1-activated genes
SKN−1 (L2)
SKN−1 (L1)
FOS−1 (L2)
NHR−28 (L4)
94 others
0 5 10 15 20
(-log10(p-value))
C
unc-62-activated genes
UNC-62 (YA)
UNC-62 (L1)
UNC-62 (L2)
UNC-62 (L3)
BLMP-1 (L1)
93 others
-2 -1 0 1 2 3 4 5
(-log10(p-value))
D
skn-1-activated genes
(top 500 binding sites)
SKN−1 (L1)
SKN−1 (L2)
96 others
-2 0 2 4 6 8
(-log10(p-value))

Figure 6

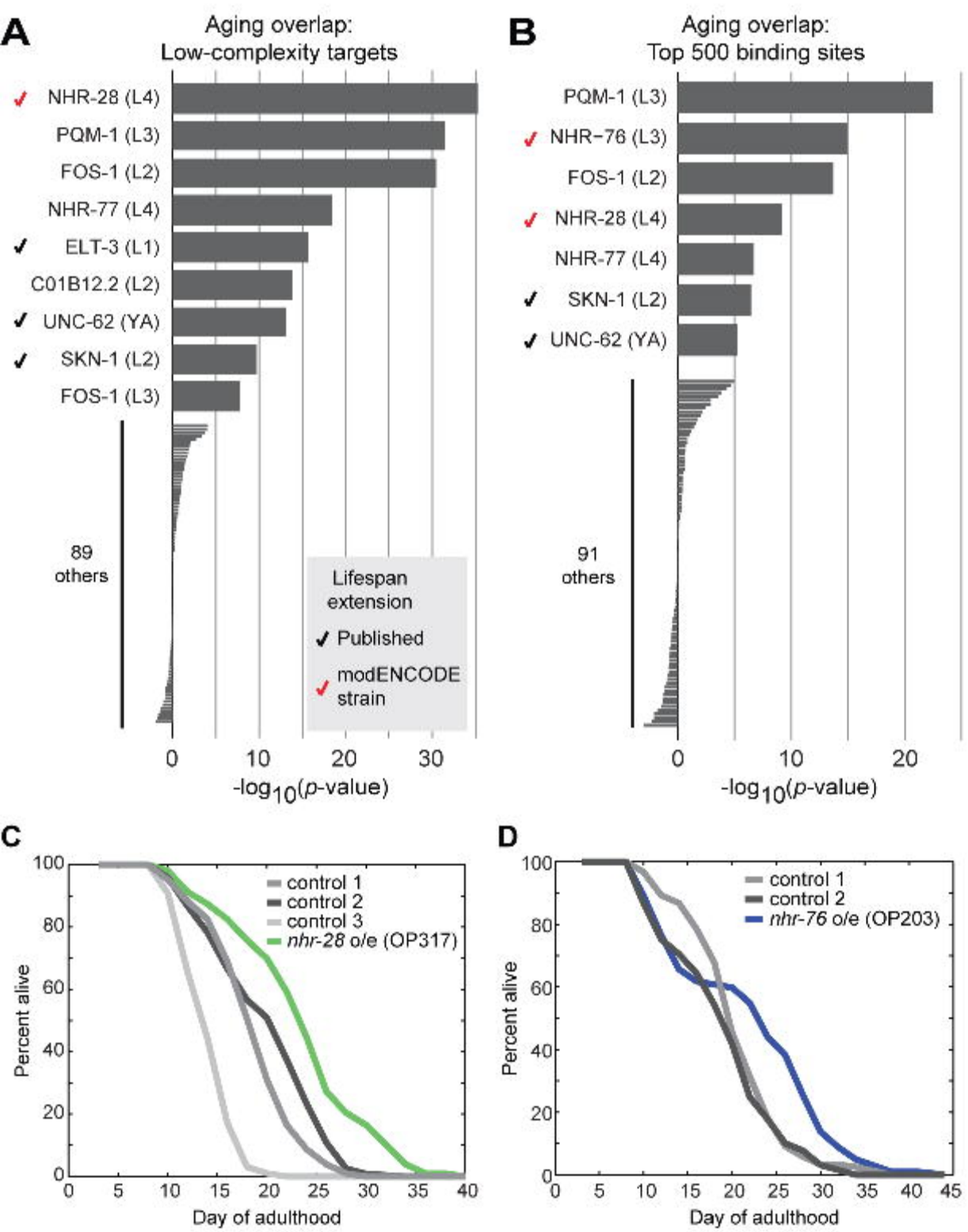
A
Aging overlap:
Low-complexity targets
NHR-28 (L4)
PQM-1 (L3)
FOS-1 (L2)
NHR-77 (L4)
ELT-3 (L1)
C01B12.2 (L2)
UNC-62 (YA)
SKN-1 (L2)
FOS-1 (L3)
89
others
Lifespan
extension
Published
modENCODE
strain
0
10
20
30
-log10(p-value)
B
Aging overlap:
Top 500 binding sites
PQM-1 (L3)
NHR-76 (L3)
FOS-1 (L2)
NHR-28 (L4)
NHR-77 (L4)
SKN-1 (L2)
UNC-62 (YA)
91
others
0
10
20
-log10(p-value)
C
control 1
control 2
control 3
nhr-28 o/e (OP317)
Percent alive
Day of adulthood
D
control 1
control 2
nhr-76 o/e (OP203)
Percent alive
Day of adulthood

Supplemental Figure 1

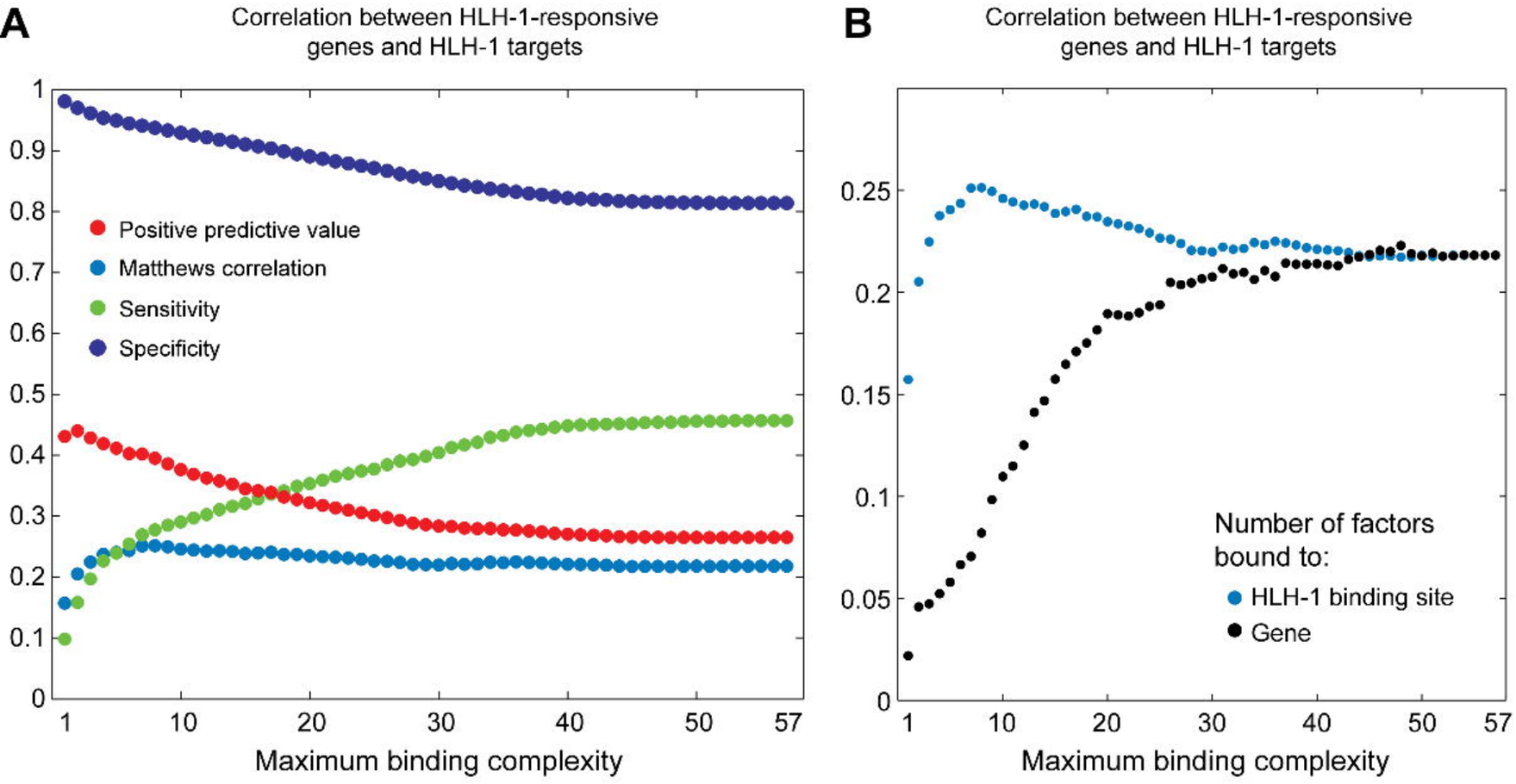

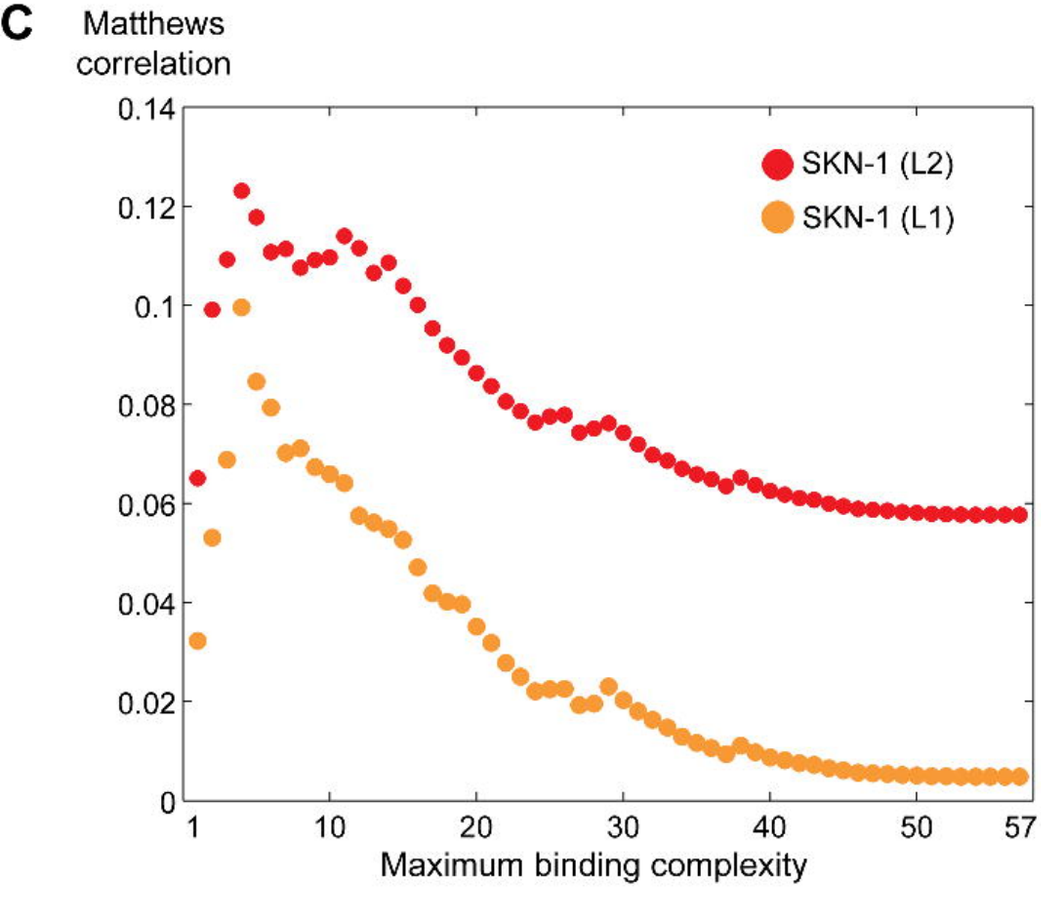

Supplemental Figure 2

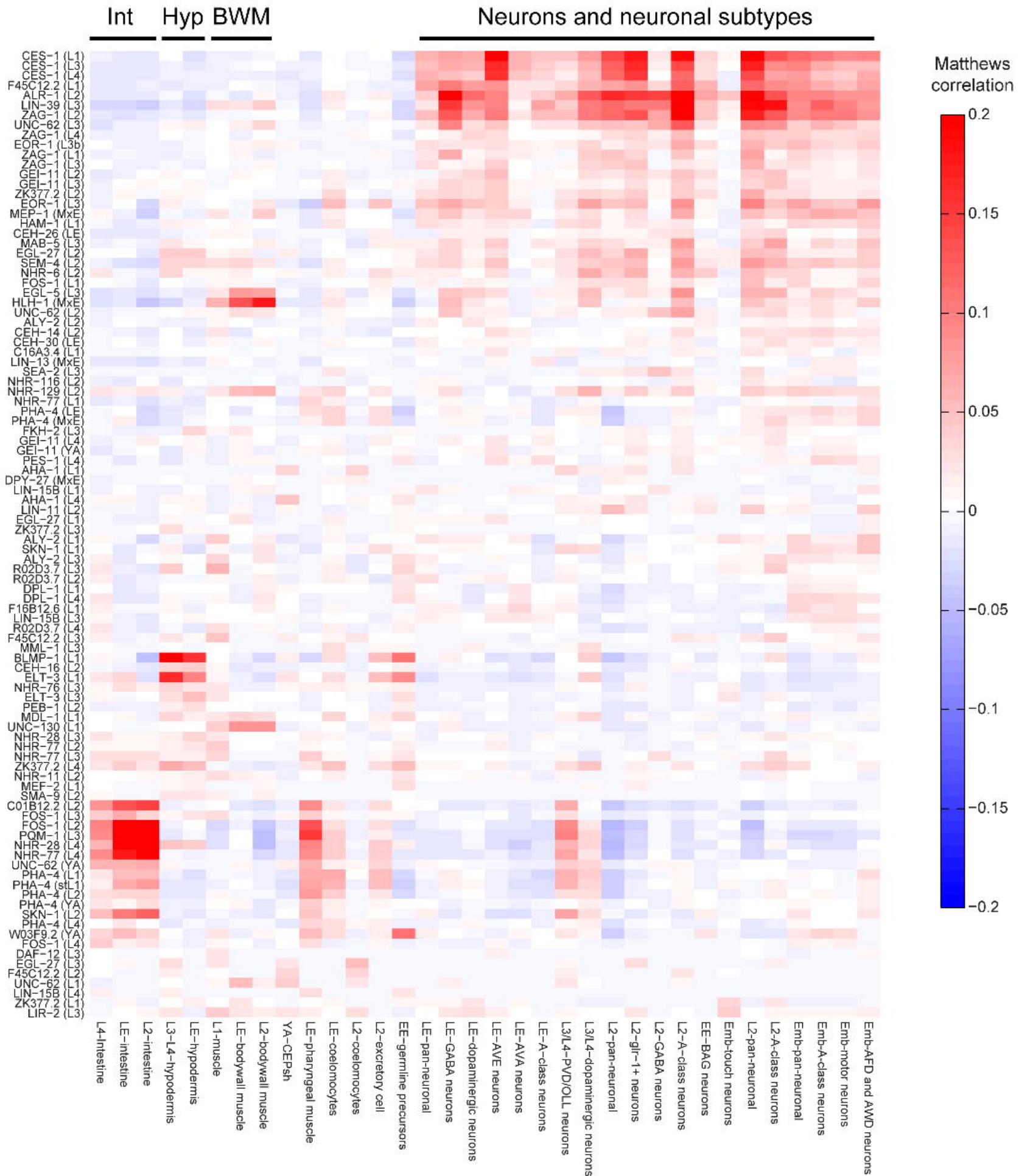

Supplemental Figure 3

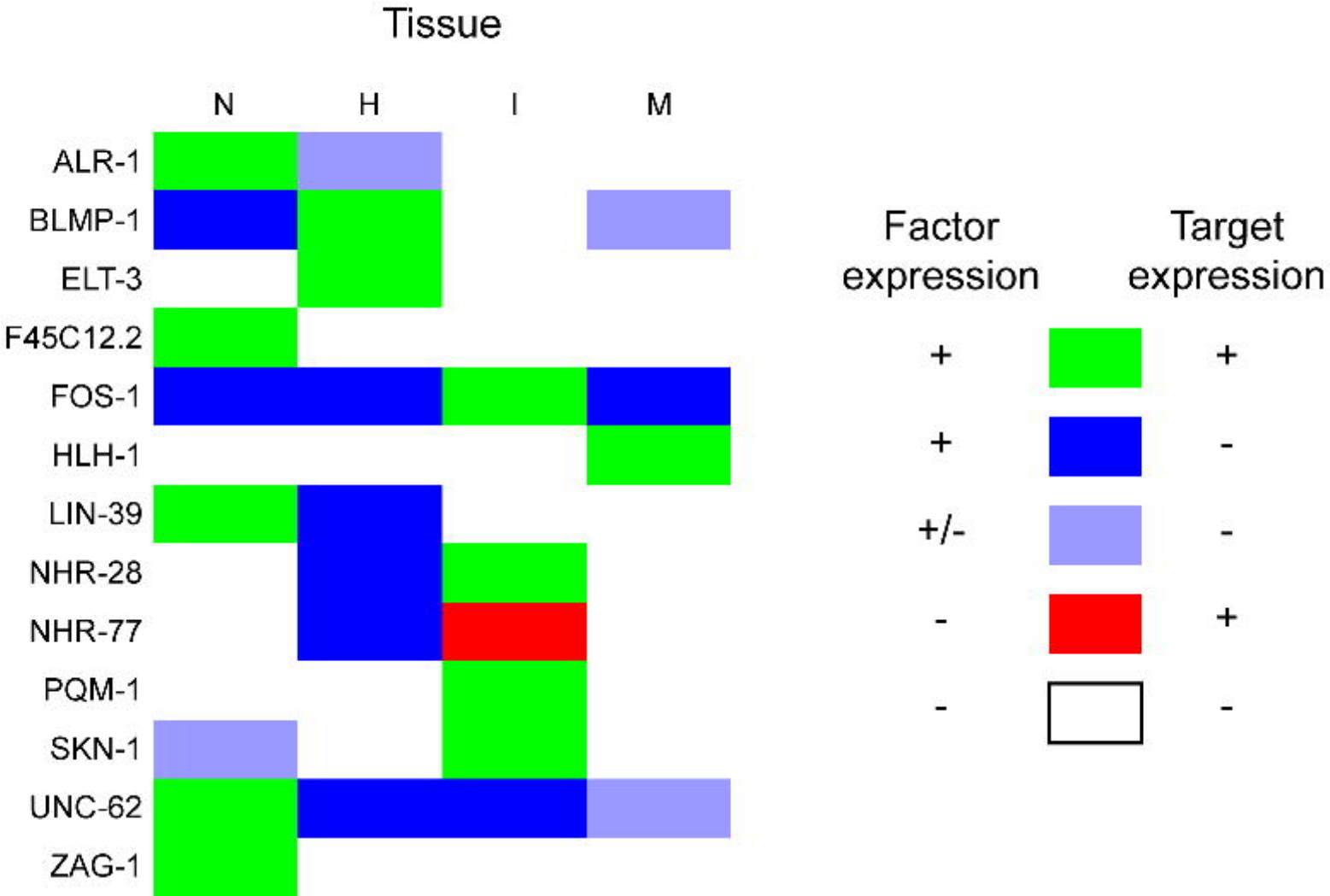

Supplemental Figure 4

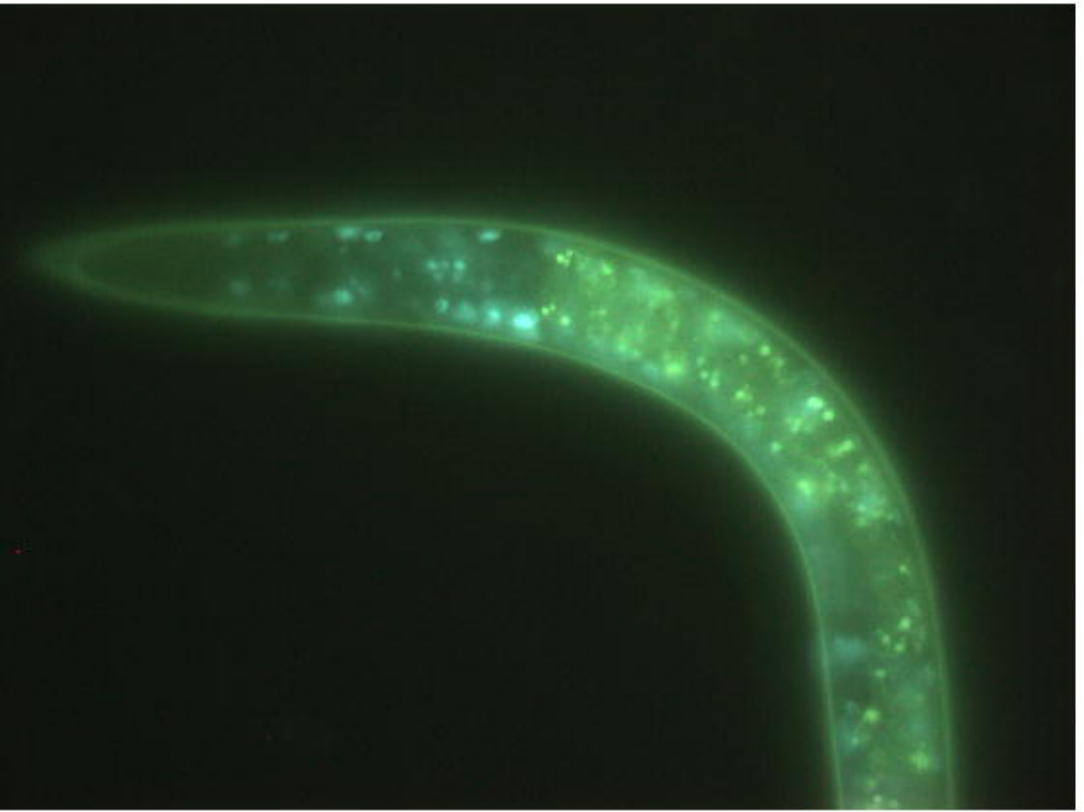

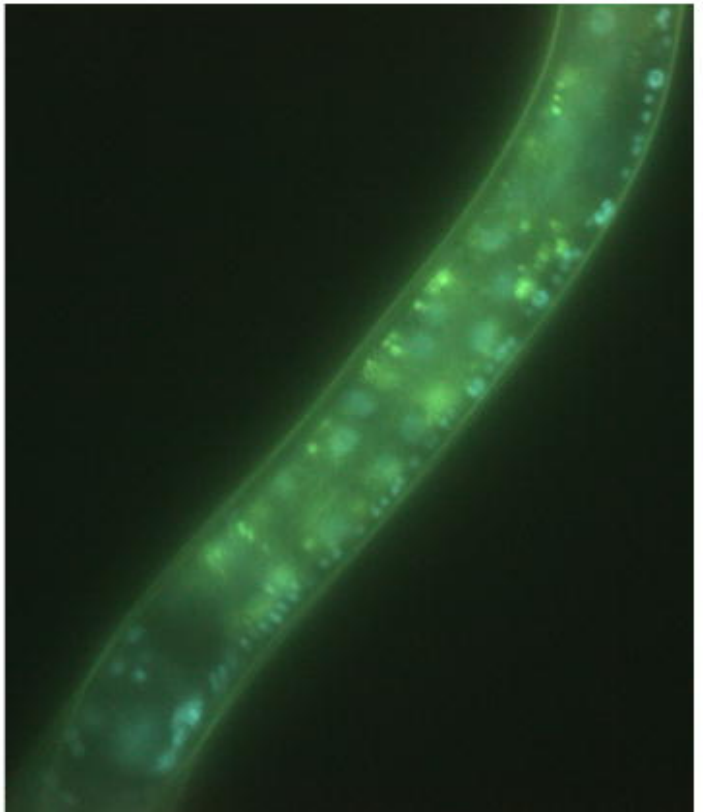

Supplemental Figure 5